Universidade de Aveiro Departamento de Ciências Médicas
2016

Ana Marlene Neto Marafona

O novo complexo LAP1:TRF2 está associado a danos no DNA

The novel LAP1:TRF2 complex is associated to DNA damage

Universidade de Aveiro Departamento de Ciências Médicas
2016

Ana Marlene Neto Marafona

O novo complexo LAP1:TRF2 está associado a respostas a danos no DNA

The novel LAP1:TRF2 complex is associated to DNA damage

Dissertação apresentada à Universidade de Aveiro para cumprimento dos requisitos necessários à obtenção do grau de Mestre em Biomedicina Molecular, realizada sob a orientação científica da Professora Doutora Sandra Maria Tavares da Costa Rebelo, Professora Auxiliar Convidada do Departamento de Ciências Médicas da Universidade de Aveiro

Este trabalho foi financiado pelo iBiMED (Instituto de Biomedicina-UID/BIM/04501/2013) e contou com o apoio do grupo de Neurociências e Sinalização Celular do iBiMED, Departamento de Ciências Médicas, Universidade de Aveiro.

Dedico esta dissertação à memória de duas pessoas que marcaram muito a minha vida. Aos meus tios um muito obrigado por toda a educação e ensinamentos transmitidos.

o júri

Presidente

Professora Doutora Odete Abreu Beirão da Cruz e Silva
Professora Auxiliar com Agregação do Departamento de Ciências Médicas da Universidade de Aveiro

Professora Doutora Etelvina Maria de Almeida Paula Figueira
Professora Auxiliar do Departamento de Biologia da Universidade de Aveiro

Professora Doutora Sandra Maria Tavares da Costa Rebelo
Professora Auxiliar Convidada do Departamento de Ciências Médicas da Universidade de Aveiro

Agradecimentos

À minha orientadora, Professora Doutora Sandra Rebelo, agradeço por toda a dedicação, amizade, disponibilidade e apoio. Um obrigado do fundo do coração por todos os ensinamentos transmitidos.

A todos os meus colegas do Laboratório de Neurociências e Sinalização, por todos os conselhos, amizade, apoio e ensinamentos transmitidos. Um agradecimento à Oli, à Rochinha e à Soraia.

Um muito obrigado ao Roberto por nunca me ter negado um pedido de ajuda e pelos seus conselhos sábios.

A todas as minhas colegas do mestrado, em especial à Carolina e à Sónia. Obrigada pelo companheirismo, apoio e sobretudo pela amizade.

A todas as minhas colegas da R 2.1A, em especial à Tininha, Vânia, Sílvia, Ana, Sara e Vanessa. Obrigada pela vossa amizade e por terem ouvido sempre os meus desabafos.

À Filipa um muito obrigado pela cooperação, paciência, amizade e por todos os ensinamentos que me transmitiste.

À Joana Serrano um obrigado do fundo do coração, por toda a dedicação, paciência, amizade e companheirismo. Obrigada por todos os ensinamentos transmitidos e obrigada por me teres mostrado o verdadeiro significado da "Ciência".

Ao Renato, um obrigado do fundo do meu coração pelo amor, por todos os conselhos, apoio e por teres acreditado sempre nas minhas capacidades! Obrigada por toda a força, ternura, coragem e confiança que me transmitiste!

Aos meus pais, avó e irmãos, um obrigado por toda a dedicação, amor, apoio e sobretudo por terem acreditado em mim!

palavras-chave

Proteína 1 associada com a lâmina (LAP1), Membrana nuclear interna (INM), Mutação da Ataxia Telangiectasia (ATM), Factor 2 de ligação às repetições teloméricas (TRF2), Proteína 1 activadora repressora (RAP1), quebras de DNA de cadeia dupla (DSBs), Membro da família da histona 2A (γ-H2AX), Involucro nuclear (NE)

Resumo

Proteína 1 associada com a lâmina (LAP1) é uma proteína integral da membrana do tipo II localizada na membrana nuclear interna (INM). O papel da LAP1 não é inteiramente sabido, no entanto esta proteína tem sido associada a algumas funções celulares devido às suas interações com as lâminas, proteína fosfatase 1 (PP1), emerina e torsinA. Além disso, novos putativos interactores da LAP1 estão a surgir. Um recente estudo do nosso grupo permitiu a identificação de vários novos putativos interactores da LAP1 envolvidos na sinalização dos telómeros e em respostas a danos no DNA, nomeadamente a mutação da ataxia telangiectasia (ATM), fator 2 de ligação às repetições teloméricas (TRF2), proteína 1 ativadora repressora (RAP1), fator homólogo 1 de interação com a RAP1 (RIF1), proteína 1 do checkpoint do fuso mitótico (MAD2L1) e a proteína de ligação à proteína 1 do checkpoint do fuso mitótico (MAD2L1BP). As interações proteína-proteína são cruciais no estudo das vias de sinalização. Neste estudo, a TRF2 foi identificada como uma nova proteína interatora da LAP1 utilizando tanto co-immunoprecipitação como metodologias baseadas em espectrometria de massa. Para determinar a relevância funcional do novo complexo LAP1:TRF2, células HeLa foram submetidas a danos no DNA através do peróxido de hidrogénio (H_20_2), nomeadamente a quebras de DNA de cadeia dupla (DSBs). Em resposta a DSBs, os níveis de expressão da LAP1 e da TRF2 estavam significativamente reduzidos. A fosforilação do membro da família da histona 2A (γ-H2AX) que é considerado um biomarcador de DSBs foi também avaliada. Em resposta a danos no DNA, a LAP1 não só co-localiza com a γ-H2AX em alguns pontos específicos perto do invólucro nuclear (EN) e núcleo, mas também com TRF2 na periferia nuclear. Além disso, a LAP1 e a TRF2 têm sido reportadas como proteínas cruciais na progressão do ciclo celular. Por isso, decidimos prosseguir com esta questão. Quando o EN é remontado, o complexo está localizado principalmente em regiões especificas do EN, evidenciado que a TRF2 permite a ligação dos cromossomas à membrana do NE em células somáticas. Como conclusão, os nossos resultados são de uma importância suprema, uma vez que novas descobertas funcionais relativas ao novo complexo LAP1:TRF2 foram alcançadas, particularmente relacionadas com respostas a danos no DNA e progressão do ciclo celular.

keywords

Lamin associated protein 1 (LAP1), Inner nuclear membrane (INM), Ataxia-telangiectasia mutated (ATM), Telomeric repeat binding factor 2 (TRF2), Repressor Activator Protein 1 (RAP1), Double-stranded breaks (DSBs), Histone 2A family member (γ-H2AX), nuclear envelope (NE)

abstract

Lamin associated protein 1 (LAP1) is a type II integral membrane protein located at the inner nuclear membrane (INM). The role of LAP1 remains poorly understand, however, this protein has been associated with several cellular functions due to its interactions with lamins, phosphatase protein 1 (PP1), emerin and torsinA. Moreover, novel putative LAP1 interactors are emerging. A recent study from our group allowed the identification of several novel putative LAP1 interactors involved in telomere signaling and DNA damage responses, namely Ataxia-telangiectasia mutated (ATM), Telomeric repeat binding factor 2 (TRF2), Repressor Activator Protein 1 (RAP1), RAP1 interacting factor 1 homologue (RIF1), Mitotic arrest deficient-like1 (MAD2L1) and Mitotic arrest deficient-like1 binding protein (MAD2L1BP). Protein-protein interactions are crucial in the study of signaling pathways. In this study, TRF2 was identified as a novel LAP1 binding protein using both co-immunoprecipitations and mass spectrometry based methodologies. To determine the functional relevance of the novel complex LAP1:TRF2, HeLa cells were subjected to DNA damage using hydrogen peroxide (H_2O_2), namely double-stranded breaks (DSBs). In response to DSBs, the expression levels of LAP1 and TRF2 were significantly reduced. The phosphorylation of Histone 2A family member (γ-H2AX) that is considered the hallmark of DSBs was also evaluated. Upon DNA damage, LAP1 not only co-localizes with γ-H2AX in some specific points near nuclear envelope (NE) and nucleus, but also with TRF2 in the nuclear periphery. Moreover, LAP1 and TRF2 have been reported to be crucial for cell cycle progression. Therefore, we decided to pursued this issue. When the NE is reassembled, the complex is located mainly in specific regions of the NE, evidencing that TRF2 allows the attachment of chromosomes to NE membrane in somatic cells. In conclusion, our results are of paramount importance since novel functional insights regarding the novel LAP1:TRF2 complex were achieved particularly related with DNA damage response and cell cycle progression.

List of Contents

List of Abbreviations

53BP1	P53-binding protein 1
AAA+	ATPase Associated with a variety of cellular activities
AAs	Antibiotic/ antimitotic mix
ALT	Alternative Lengthening of Telomeres
ATM	Ataxia-telangiectasia mutated
ATR	Ataxia-telangiectasia and Rad 3-reduted
BAF	Barrier-to-autointegration factor
BCA	Bicinchoninic acid
BRCA1	Breast and ovarian cancer locus 1
BLM	Bloom syndrome protein
BSA	Bovine Serum Albumin
CDK	Cyclin-dependent kinase
CHK2	Checkpoint kinase 2
Co- IP	Co-Immunoprecipitation
DAPI	4',6-diamidino-2-phenylindole
DMEM	Dulbecco's Minimum Essential Media
DNA	Deoxyribonucleic acid
DNA-PKcs	DNA-dependent protein kinase catalytic subunit
DSB	Double stranded break
DT	Doubling time

dsDNA	double-stranded DNA
ECL	Enhanced Chemiluminescence
EDMD	Emery-Dreifuss muscular dystrophy
EDTA	Ethylenediaminetetraacetic acid
ER	Endoplasmic Reticulum
FANCD2	Fanconi Anemia Complementation Group D2
FBS	Fetal Bovine Serum
FG	Phenylalanine-Glycine
H_20_2	Hydrogen Peroxide
H2AX	Histone 2A family member
HDR	Homology-directed repair
Hp1	Heterochromatin protein 1
HRP	Horseradish Peroxidase
HPLC-MS	High performance liquid chromatography-mass spectrometry
HR	Homologue Recombination
ICC	Immunocytochemistry
IgG	Immunoglobulin
INM	Inner Nuclear Membrane
KASH	Klarsicht/ ANC-1/ Syne Homology
LAP1	Lamina associated polypeptide 1
LAP2	Lamina associated polypeptide 2
LAPs	Lamina associated polypeptides
LB	Loading buffer
LBR	Lamina B receptor

LINC	Linker of nucleoskeleton and cytoskeleton
MAD2L1	MAD2 mitotic arrest deficient-like 1
MAD2L1BP	MAD2 mitotic arrest deficient-like 1 binding protein
MDC1	DNA damage checkpoint protein 1
MEM	Minimum Essential Media
MRN Complex	MRE11-RAD50-NBS1 Complex
NE	Nuclear Envelope
Nesprin	Nuclear envelope spectrin repeat
NHEJ	Non-homologue end-joining
NPC	Nuclear Pore Complexes
Okadaic acid	OA
ONM	Outer Nuclear Membrane
PBS	Phosphate-buffered saline solution
PFA	Paraformaldehyde
PNS	Perinuclear Space
POMs	Pore Membrane proteins
POT1	Protein protection of telomeres 1
PP1	Protein Phosphatase 1
PP2A	Protein Phosphatase 2A
RAP1	Repressor activator protein 1
RBM	RAP1 binding motif
RCT	RAP1 C-terminal domain
RER	Rough Endoplasmic Reticulum
RIF1	Rap1 interacting factor 1

ROS	Reactive oxygen species
SDS-PAGE	Sodium Dodecyl Sulphate-Polyacrylamide gel electrophoresis
SEM	Standard error
SMC1	Structural maintenance of chromosomes protein 1A
SR	Spectrin-repeat
ssDNA	Single-stranded DNA
TB	Trypan blue
TBS-T	Tris-buffered saline-Tween
TERC	RNA template
TERRA	Telomeric repeat-containing RNA
TERT	Telomerase reverse transcriptase
TIN2	TRF1 interacting nuclear factor 2
TM	Transmembrane
TPP1	Tripeptidyl peptidase 1
TRF1	Telomeric repeat binding factor 1
TRF2	Telomeric repeat binding factor 2
TRF2IP	Telomeric repeat binding factor 2 interacting protein
WB	Western Blot
WRN	Werner syndrome protein

Introduction

1. Introduction

1.1 Organization of the Nuclear Envelope

The nuclear envelope (NE) is a highly organized double membrane that separates the nucleus from the cytoplasm in eukaryotic cells. It is constituted by the outer (ONM) and the inner nuclear membranes (INM) that are interconnected through nuclear pore complexes (NPCs) and nuclear lamins (Figure 1). The NPCs regulate the passage of macromolecules between the nucleus and cytoplasm and are associated with the nuclear laminas[1]. The ONM is coated with ribosomes and it is continuous with the endoplasmic reticulum (ER), while the INM is constituted by membrane proteins and phospholipids, and it is closely associated with chromatin (Figure 1). The INM and the ONM are separated by a perinuclear space (PNS) and are functionally unique due to enrichment of distinct integral membrane proteins[2,3] (Figure 1). The nuclear lamina is a meshwork of intermediate filaments juxtaposed to the INM and is composed by lamins[4]. Lamins are type-V intermediate filament proteins[5]. The nuclear lamins are composed of A- and B-type lamins, which play important roles in nuclear stability, chromatin function and gene expression[6]. There are three genes encoding nuclear lamins, *LMNA*, *LMNB1* and *LMNB2*. The *LMNA* gene encode for A-type lamins, while the *LMNB1* and *LMNB2* encode for B-type lamins (lamin B1, B2, and B3). A-type lamins are expressed in a specific tissue manner during differentiation, while the B-type lamins are expressed in all cell types[7].

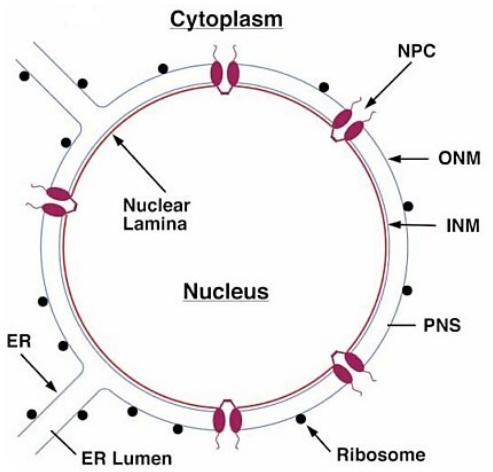

Figure 1. **Structure of NE.** The NE is a highly complex organelle composed by a double membrane which separates the nucleus from cytoplasm. The NE is constituted by the INM, ONM, nuclear lamins and

NPCs. The INM and ONM is separated by PNS. The ONM is continuous with ER and it is coated with ribosomes. The INM maintains interactions with chromatin and it is constituted by membrane proteins. The nuclear lamins are intermediate filaments located in INM and are constituted by lamin proteins. The NPCs regulate the passage of macromolecules between the nucleus and the cytoplasm. Adapted from[2].

1.1.1 Nuclear envelope proteins

The NE proteins can be classified according to their position in the NE. The first group is constituted by trans-nuclear membrane proteins in the NPCs, the second group is characterized by integral nuclear membrane proteins that are localized in the INM through transmembrane domains and stabilizing interactions with lamins and chromatin (for example, Lamin B Receptor (LBR), Lamina Associated Polypeptide 1 (LAP1), Lamina Associated Polypeptide 2 (LAP2), emerin, SUN and MAN1)) and finally, the third group is constituted by proteins which are located in the ONM, for instance, nuclear envelope spectrin repeat (nesprin)-1, -2, -3 and 4[6,8] (Figure 2).

The ONM and INM proteins are known to form complexes that bridge across the perinuclear space. These luminal proteinaceous bridges establish physical connections between the chromatin and cytoskeleton. They are therefore relevant in mechanisms as transcription, replication and deoxyribonucleic acid (DNA) repair[6].

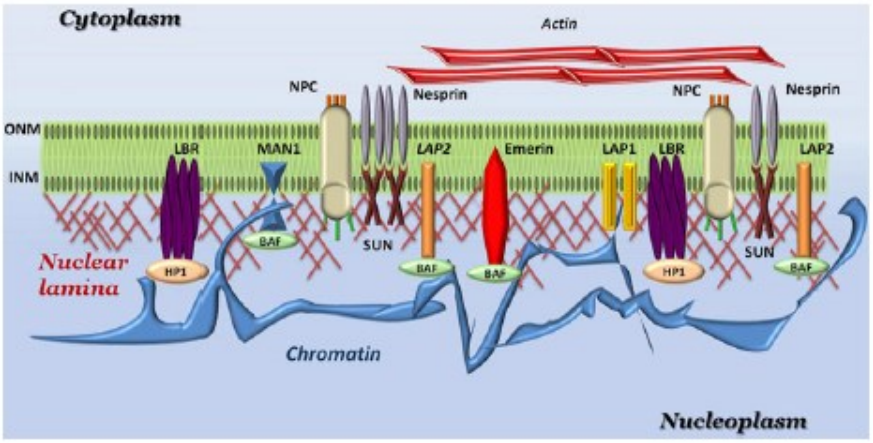

Figure 2. **NE proteins.** NE proteins are classified according to their position in NE: i) NPCs proteins, ii) INM proteins (LBR, MAN1, SUN, LAP2, emerin, and LAP1) and iii) ONM proteins (nesprins). Reproduced from[15].

1.1.1.1 Nuclear Pore Complexes

The NPCs are protein complexes responsible for molecular trafficking between the nucleus and the cytoplasm of eukaryotic cells and they are embedded in the NE double-membrane. The NPCs have a cylindrical geometry and a molecular weight between 60 to 100 MDa[9,10]. Structurally, the NPCs are constituted by cytoplasmic filaments, the central core and the nuclear basket (Figure 3). The central core is constituted by five concentric cylinders which are constituted by four substructures: pore membrane proteins (POMs), coat nucleoporins, adaptor nucleoporins, channel nucleoporins and phenylalanine-glycine (FG) repeats[11] (Figure 3).

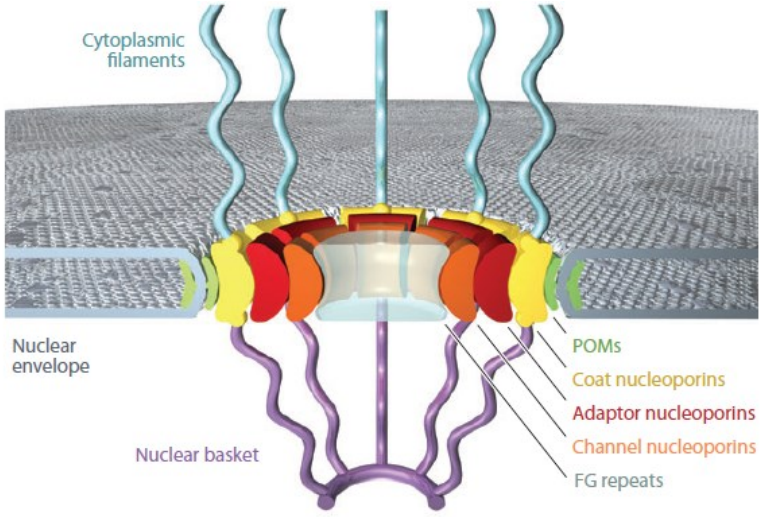

Figure 3. **Structure of NPCs.** The NPCs are protein complexes constituted by cytoplasmic filaments (blue), the central core and the nuclear basket (purple). The central core has five substructures: pore membrane proteins (POMS), represented in green; coat nucleoporins, represented in yellow; adaptor nucleoporins, represented in red; channel nucleoporins, represented in orange and Phenylalanine-glycine (FG) repeats, represented in blue. Adapted from[11].

The NPCs are constituted by a set of 30 proteins termed nucleoporins or Nups. The Nups are composed by three structural units: α-helical regions, β-propellers and FG repeats that mediate nucleocytoplasmic transport of molecules that cross the NE[12,11,13]. According to their localization within the NPCs, the Nups can be classified into six categories: i) integral membrane protein of the POMs domain, ii) membrane-apposed coat nucleoporins, iii) adaptor nucleoporins, iv) channel nucleoporins, v) nuclear basket nucleoporins and vi) cytoplasmic filament nucleoporins[11]. The Nups are essential for cell division, transcriptional

activation and regulation of the protein and RNA transport between the nucleus and the cytoplasm[14].

1.1.1.2 Inner Nuclear Membrane

The research into the INM is highly relevant for human health, since the INM is a structure enriched in proteins that are important for many cellular processes, including maintenance of the nuclear structure, chromosome organization, DNA repair and transcriptional control[15,16]. The LBR is an INM protein encoded by *LBR* gene that belongs to the sterol reductase family[8] (Figure 4). It binds to emerin and heterochromatin protein 1 (Hp1), through its NH2-terminal domain[15,17].

Emerin is a type II integral membrane protein encoded by *EDM* gene[18] (Figure 4). Emerin is involved in multiple biological processes, such as direct and indirect regulation of transcription factors activity, nucleo-cytoskeletal mechanotransduction, maintenance of the nuclear structure, chromatin condensation and epigenetics modifications. This protein has the capacity to attenuate Wnt signaling, since it binds to β-catenin and inhibits its nuclear accumulation, influencing thereby adipogenesis. Furthermore, emerin binds to and inhibits Lmo7 transcription factor that is expressed at high levels in the muscle and heart tissues, regulating a variety of muscle-related genes[19, 20].

MAN1 is a protein constituted by two transmembrane spanning domains, the NH2- and the COOH-terminal nucleoplasmic domains[21,22] (Figure 4). This protein plays a fundamental role in chromosome segregation, cell division and early development. Several INM proteins together with MAN1 contribute to the nuclear assembly by re-associating with chromatin and facilitating the conversion of tubular ER into the sheet ER to reform the NE immediately after mitosis[22,23]. Furthermore, MAN1 shares a conserved globular domain with two INM proteins, namely LAP2 and emerin, designated as the LEM domain (LAP2, emerin, MAN1). This domain binds to lamins and play a role in tethering chromatin through BAF (barrier-to-autointegration factor). These mutual binding partners (LEM-domain proteins, lamins, BAF) are very important in the reassembly of the NE and lamin networks around chromatin after mitosis[6,19,24,25].

LAP1 is a type II integral membrane protein encoded by the *TOR1AIP1* gene and interacts with lamins, torsinA, protein phosphatase 1 (PP1) and emerin, providing a pivotal

mechanism for transducing signal across the INM[26] (Figure 4). A detailed description of this protein is available below (section 1.2).

LAP2 is also a type II integral membrane that belongs to the thymopoietins family. This protein plays an important role in NE organization due to its binding to lamins and chromosomes. LAP2 is additionally involved in the association between chromosome-membranes[27,28] (Figure 4).

SUN-domain proteins (SUN 1 and SUN 2) together with nesprins form the LINC complex (Linker of Nucleoskeleton and Cytoskeleton). The SUN proteins link the nuclear lamina with the actin and tubulin cytoskeleton and play a role in nuclear positioning and cellular migration[29] (Figure 2).

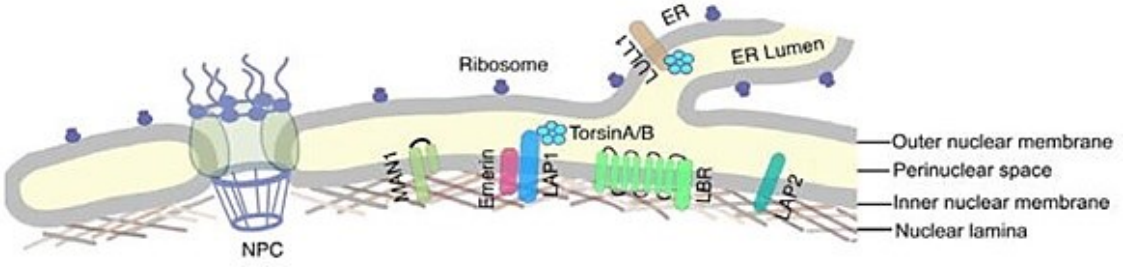

Figure 4. **Schematic view of the INM proteins.** The inner nuclear membrane is a structure enriched with membrane proteins that are crucial for many biological processes. LBR binds to emerin and chromatin associated proteins, like HP1. The LEM domain-containing proteins (LAP2, emerin, MAN1) are known to bind to chromatin associated proteins, like the barrier autointegration factor (BAF). Sun proteins interact through the PNS with nesprins and together forms the LINC complex. LAP1 interacts with lamins, torsinA, PP1 and emerin while LAP2 binds to lamins and chromosomes. Reproduced from[36].

1.1.1.3 Outer Nuclear Membrane

Nesprins are vertebrate spectrin-repeat (SR)-containing proteins and are localized in ONM. These proteins are composed by a conserved C-terminal Klarsicht/ANC-1/Syne Homology (KASH) domain and are key components of the LINC complex[30].

In the cytoplasm, nesprins bind to cytoskeletal elements and they are projected into the PNS, where they interact with INM proteins termed SUN proteins. The LINC complex is involved in many cellular functions, including nuclear positioning, mechanotransduction, cell division, organization of the cytoskeleton, polarity/migration, cell signaling, cell stiffness, nuclear migration, organelle positioning, ciliogenesis, meiosis, chromatin

organization, chromosome movement, cell/nuclear architecture and DNA damage repair[20,30,31].

In mammals, four KASH-domain proteins were identified, including nesprin-1, -2, -3 and -4. The nesprins-1 and -2 are known to stabilize connections with the actin cytoskeleton and co-localize with LAP1, emerin and lamins at the NE[30,32,33]. Nesprins-3 binds to plectin, a protein that is associated with a filaments system: actin filaments, intermediate filaments and microtubules[34]. Nesprin-4 is present in the NE of the salivary gland, exocrine pancreas, bulbourethral gland and mammary tissue[35].

1.2 Lamina Associated Polypeptide 1

1.2.1 Physiological role of LAP1

As mentioned above, LAP1 is a type II integral membrane protein located in INM. LAP1 is encoded by the *TOR1AIP1* gene. Members of the LAP1 family were identified using a monoclonal antibody against lamina-enriched fractions of rat liver nuclei. The antibody recognized three polypeptides in rat liver NEs, LAP1A (75 kDa), LAP1B (68 kDa) and LAP1C (56 kDa). These three LAP1 isoforms result from alternative splicing of the *TOR1AIP1* gene[26,36,37]. Afterward, the same isoforms were described in mouse[27]. In humans, the full-length cDNA of LAP1B was isolated from an expression library of HeLa cells. Additionally, a splice variant of LAP1B was identified, which differs from the previously identified LAP1B by the delection of three nucleotides (CAG) from exon 3, resulting in the removal of one alanine in the LAP1B protein[38]. Recently, a new LAP1 isoform was identified in humans and was named LAP1C. LAP1C is abundant in both human cell lines and in tissues[38]. Briefly, the expression of both LAP1B and LAP1C isoforms is tissue specific, in testis and ovary have a similar expression, but in tissues like lung, kidney and spleen LAP1C is more abundant. Moreover, in brain and heart the expression of human LAP1B was higher than LAP1C[27,38].

Structurally, both LAP1B and LAP1C have a nucleoplasmic N-terminal domain, a single transmembrane (TM) domain and a luminal C-terminal domain that is located at the PNS. However, LAP1C has putatively a truncated N-terminal domain[26,38].

To date the precise physiological function of LAP1 is unknown, however several functions have been ascribed to LAP1 since it binds to several proteins. Among them are lamins, PP1, torsinA and emerin. LAP1 binds directly to lamin A/C and lamin B[39]. During

interphase and mitosis the LAP1 is associated with the maintenance of the NE architecture through its binding to lamins and chromatin[38, 40] (Figure 5). LAP1B is a novel PP1 binding protein and it was established in our group that LAP1 is a novel PP1 substrate, with PP1 dephosphorylating LAP1's Ser306 and Ser310[37,38]. LAP1 also interacts with torsinA (Figure 5), a protein with 332 amino acids that belongs to the AAA-ATPase (ATPase Associated with a variety of cellular Activities) family of chaperones. This interaction it is important for NE localization of torsinA, regulation of torsinA ATPase activity and NE dynamics[41–43]. Emerin was also identified as a LAP1 interacting protein. The interaction between these two proteins is mediated by LAP1 nucleoplasmic domain and it is relevant to NE integrity maintenance and skeletal muscle maintenance[44].

The protein phosphorylation is an important mechanism that regulates the cell cycle progression[40] (Figure 5). During the mitosis, LAP1 is phosphorylated by several kinases that regulate the cell cycle, respectively on Ser143 by cyclin-dependent kinase (CDK) and on Ser164 by ataxia-telangiectasia mutated (ATM) and ataxia-telangiectasia and Rad 3-related (ATR)[40]. LAP1 is a protein that has a key role in the cell cycle progression and in the maintenance of the NE. During mitosis, in organisms such as yeast, the NE remains intact while in other organisms, such as *Caenorhabditis elegans* and *Drosophila melanogaster*, it is disrupted at later stages of mitosis[40]. In eukaryotes, the NE is completely disassembled at the beginning of mitosis and reassembled at the culmination of mitosis. The NE disassembled is characterized by disassembly of NPCs, depolymerization of lamins and spreading of NE soluble components and INM proteins to the cytoplasm and ER, while NE reassembly is characterized by an increase of INM proteins and lamins on the decondensing chromatin, lamin polymerization and NPCs assembly[40]. One of the first INM proteins identified was LAP1[40]. During mitosis, LAP1 is associated to reassembly of NE, assembly of the mitotic spindle and co-localizes with α-tubulin and γ- tubulin, markers of microtubules stability and microtubule organizing center respectively. In interphasic cells, LAP1 appears to be associated with lamins and chromosomes in the INM. In prometaphase, LAP1 loses its association with lamins and chromosomes and it is found redistributed in ER, contributing to the NE breakdown. In anaphase, LAP1 is located at the chromosomes surface, the mid-body (telophase) and the mitotic vesicles associated with the mitotic spindle[38, 40].

A recent bioinformatics study from our laboratory described the LAP1 interactome. Briefly, 41 LAP1 interactors were identified, among them are RAP1 interacting factor 1

(RIF1), ATM, MAD2 mitotic arrest deficient-like 1 (MAD2L1), MAD2 mitotic arrest deficient-like 1 binding protein (MAD2L1BP), Telomeric repeat binding factor 2 (TRF2) and repressor activator protein 1 (RAP1), also known by Telomeric repeat binding factor 2 interacting protein (TRF2IP). This study suggested several novel LAP1 putative functions, in addition to those already associated with LAP1, namely as regulation of response to DNA damage, nuclear membrane organization, nuclear envelope organization, cell cycle regulation, chaperone-mediated protein folding, nucleus organization, telomere maintenance, cellular component organization, telomere organization and cellular component disassembly involved in execution phase of apoptosis[45].

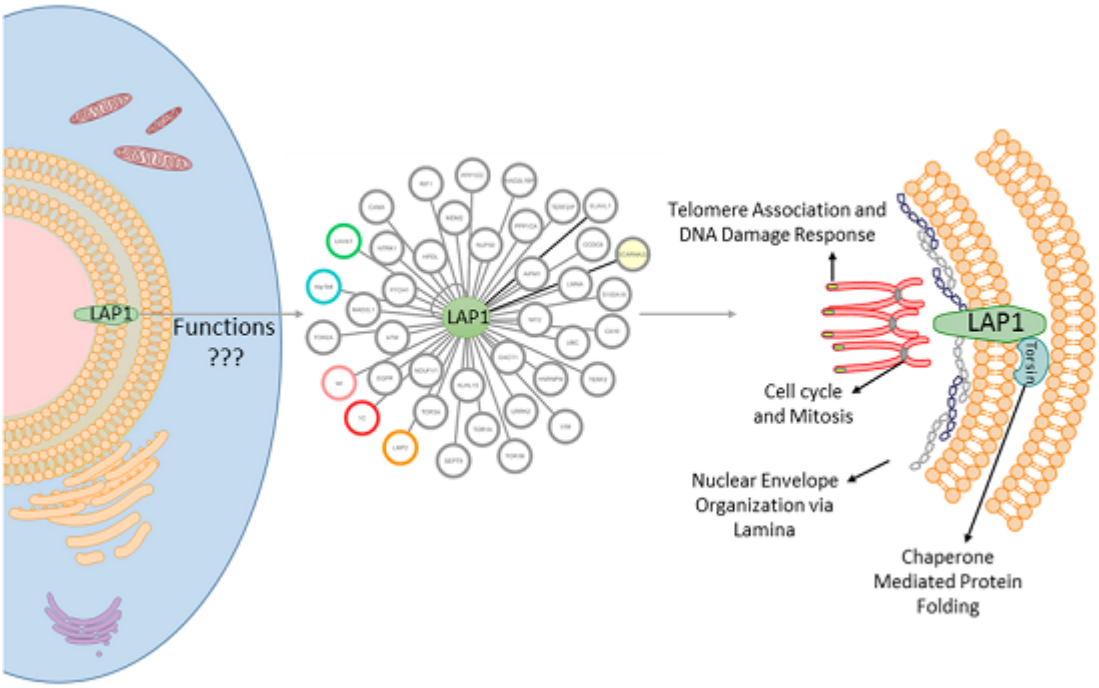

Figure 5. **Functions of LAP1.** The function of LAP1 protein is not completely known, some studies have been reported that: i) LAP1 plays an important role in maintenance of NE through its binding to lamins, ii) LAP1 binds to a torsinA protein that belongs to chaperone family, iii) LAP1 regulates the cell cycle and mitosis and during the mitosis it is dispersed at ER membranes (prometaphase), it is located at chromosomes surface (anaphase), the mid-body (telophase) and the mitotic vesicles associated with the mitotic spindle, and iv) LAP1 is also involved in telomere-association and DNA damage response. Reproduced from[45]

1.2.2 Pathological role of LAP1

To date were described four mutations in *TOR1AIP1* gene. The first mutation was reported in a consanguineous Turkish family ("Turkish" mutation). This mutation consists of a homozygous G deletion at position c.186 (c.186delG) in *TOR1AIP1* gene. The c.186delG mutation is a nucleotide delection in the first exon that is predicted to cause a frameshift and premature stop codon that subsequently results in the absence of LAP1B. This mutation leads to muscular dystrophy, a hereditary muscle disorder characterized by progressive muscular degeneration and weakness[26,44,46]. A second *TOR1AIP1* mutation results from a homozygous missense mutation (c.1448A>C) and was reported in a boy born from consanguineous healthy parents ('Moroccan' mutation). This mutation results in a change of a glutamic acid to alanine at amino acid position 482, leading to a reduced expression levels of LAP1 at the NE. This reduction of LAP1 at the NE was observed with a concomitant mislocation and aggregation of LAP1 at the ER. These patients have rapidly progressing dystonia, progressive cerebellar atrophy and dilated cardiomyopathy[26,47]. More recently, two novel pathogenic *TOR1AIP1* mutations have been reported in Australian family ("Australian" mutation). One is a frameshift mutation in exon 1 (c.127delC) of *TOR1AIP1* gene which results in a truncated protein of 58 amino acids lacking the TM domain. Consequently, these patients do not express LAP1B. The last described mutation is a missense change in exon 10 (c.1181T>C, p. L394P). Both mutations cause severe cardiac failure, musculoskeletal weakness and muscular dystrophy[48].

Additionally, LAP1 appears to be implicated in DYT1 dystonia due to its binding with torsinA. TorsinA is a member of a family of ATPase AAA+ proteins localized to the lumen of the ER. A mutation (a glutamic acid (GAG) deletion in the 3' coding region) in *TOR1A* gene that encodes for torsinA cause DYT1 dystonia, a movement disorder characterized by prolonged involuntary twitching movements[45]. This disease usually begins in childhood or adolescence and the symptoms start in the limbs with progression to other parts of the body. In normal conditions this protein is concentrated in PNS and rough endoplasmic reticulum (RER), while mutated the form is localized in PNS[37,45,46]. In NE, LAP1 interacts with torsinA and several evidences suggests that both proteins might have a combined crititical role at the NE dynamics[45,46].

As previously reported, LAP1 interacts with INM protein emerin, a protein that is associated with a neuromuscular disorder, called X-linked Emery-Dreifuss muscular

dystrophy (EDMD). This neuromuscular disorder is characterized by: 1) early contractures of the elbows, Achilles tendons and postcervical muscles, 2) slowly progressive muscle wasting and weakness, 3) cardiomyopathy with heart block[18,50–52].

1.3 DNA Damage Response

In the human body, 10^{13} cells per day are subjected to thousands of DNA lesions that are capable of blocking genome replication, transcription and can originate mutations or genomic aberrations. These lesions threaten the cell and/or organism viability if they are not repaired or if they are repaired incorrectly[53]. To repair DNA damage the cells have developed a sophisticated mechanism known as DNA damage response[54]. DNA damage signaling and repair machinery's main role is the maintenance of the genome integrity, which counteract the adverse consequences of DNA lesions and prevent their transmission to daughter cells[55].

The DNA damage response involves a set of tightly regulated steps that start with the initial detection of DNA damage, recruitment of DNA repair factors to the damage site and the repair of DNA lesions. This pathway is highly controlled by post-translational modifications (PTM), namely phosphorylation, ubiquitination, sumoylation, methylation, acetylation and others[56].

Protein phosphorylation is a well-characterized PTM mechanism associated with DNA damage response which involves the activity of proteins kinases. The phosphatidylinositol 3-kinase-related kinases (PIKKs), known as the heart of the DNA damage signaling cascade, are a family of serine/threonine proteins kinases, which include ATM, ATR and DNA-dependent protein kinase catalytic subunit (DNA-PKcs)[56,57]. The DNA damage response is mediated by proteins of PIKKs family (ATM, ATR and DNA-PKcs) and by members of the poly (ADP) ribose polymerase (PARP) family[58]. The ATM protein kinase is a 3056-amino acid polypeptide that phosphorylates its substrates in response to double-stranded breaks (DSBs). Structurally, ATM is constituted by a FAT domain (conserved among members of PIKK family, FRAP, ATR ad TRRAP), which it is located between amino acids 1966 and 2565, a phosphoinositide 3, 4-kinase (PI3K) domain, which it is located between amino acids 2609 and 2976, and FAT carboxy-terminal (FAT-C) domain, which it is located between amino acids 3024 and 3056. The amino terminal of ATM kinase (2659 amino acids) is constituted by HEAT repeats that are responsible for the

formation of a massive alpha helical scaffold[57] (Figure 6). ATM is activated upon phosphorylation of serine 1981, represented by the P in the amino-terminal region of the FAT domain. This kinase is cleaved by caspase-3 in two sites (identified by arrows in Figure 6), between amino acids 814-818 and between amino acids 860-864[57]. The ATR kinase possesses ssDNA or ssDNA/dsDNA junction DNA affinity, promoting several DNA metabolic processes that allow maintenance of the genomic integrity, namely replication fork stabilization, DNA synthesis and lesion bypass, HR, replication origin firing and cell cycle delay[54,59]. PARP1 and PARP2 are two members of PARP family involved in the DNA damage response, that are activated by SSBs and DSBs[58].

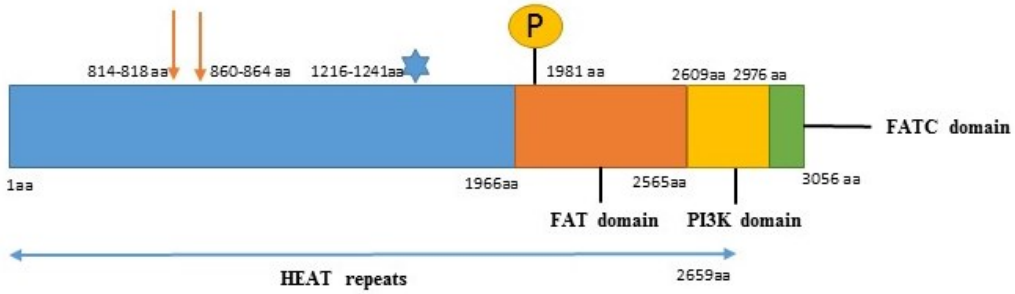

Figure 6. **Structure of ATM kinase.** The ATM is serine/threonine kinase constituted by 3056 amino acids. Structurally, it is constituted by: i) FAT domain is located between the amino acids 1966 and 2565, ii) PI3K domain is located between the amino acids 2609 and 2976 and iii) FAT-C domain is located between amino acids 3024 and 3056. The amino terminal composed by 2659 amino acids is constituted by HEAT repeats, this structure forms a massive alpha helical scaffold. ATM is activated by phosphorylation in serine 1981, indicated by the P in the amino-terminal region of the FAT domain. The two arrows indicate the position of caspase-3 cleavage between amino acids 814-818 and 860-864. The star indicates a putative zipper region between amino acids 1216 and 1241. Adapted from[57].

1.3.1 ATM-mediated DNA Damage Response

When cells are exposed to damaging agents (cellular metabolism, oxidative stress, Ultraviolet radiation (UR), Ionizing Radiation (IR) and replication errors), DSBs are originated. The DSBs can be lethal to the cell, so it is very important to cell vitality that these lesions are detected early on[58,60]. Primarily, DSBs are sensed by a protein complex termed, the MRE11-RAD50-NBS1 (MRN) complex (Figure 7)[57,61]. The MRN complex is a DNA damage response sensor, which is responsible for recruiting ATM kinase, activation of cell cycle checkpoints, effector pathways and facilitating interplay between repair mechanisms.

Mre11 binds to Nbs1, DNA and Rad50. ATM kinase phosphorylates Nbs1 at Ser343 and both Nbs1 and MRN complex are vital to full activation of ATM[57,61]. Furthermore, the ATM kinase is also auto phosphorylated at Ser1981 and consequently the inactive dimer is converted into its active monomeric form in response to DSBs[57,61] (Figure 7). The activation of ATM leads to phosphorylation and recruitment of downstream substrates, including breast and ovarian cancer locus 1 (BRCA1), p53-binding protein 1 (53BP1), histone 2A family member (H2AX), p53, Checkpoint kinase 2 (CHK2), Fanconi anemia complementation group D2 (FANCD2), structural maintenance of chromosomes protein 1A (SMC1) and Bloom's syndrome mutated 1 (BLM1)[62]. 53BP1 also sustains the DNA damage signaling through ATM activation[63] (Figure 7). BRAC1 is recruited to sites of DNA damage where it acts as a scaffold for ATM kinase activation and is involved in cell repair[57,63] (Figure 7). In response to DSBs, γ-H2AX is phosphorylated at Ser139 by ATM and it can recruit the mediator of DNA damage checkpoint protein 1 (MDC1), which in turn leads to cell repair and chromatin descondensation (Figure 7). γ-H2AX is dephosphorylated by protein phosphatase 2A (PP2A) and this mechanism facilitates DSBs repair[64]. The activation of ATM kinase also leads to phosphorylation of downstream effectors, namely the Thr68 of Chk2 kinase. The Chk2 phosphorylates the central suppressor p53, which activates the transcription of genes that participate in DNA repair, senescence, apoptosis and initiate cell cycle arrest at the G1-S boundary[56] (Figure 7). The tumor suppressor protein p53 is a sensor of cellular stress and it is involved in the regulation of cellular responses to DNA damage[65]. p53 is phosphorylated by ATM at Ser15, and this phosphorylation leads to two mechanisms: i) cell growth arrest for repair DNA damage; or ii) apoptosis if the cells cannot be capable of repair DNA damage[65,66] (Figure 7).

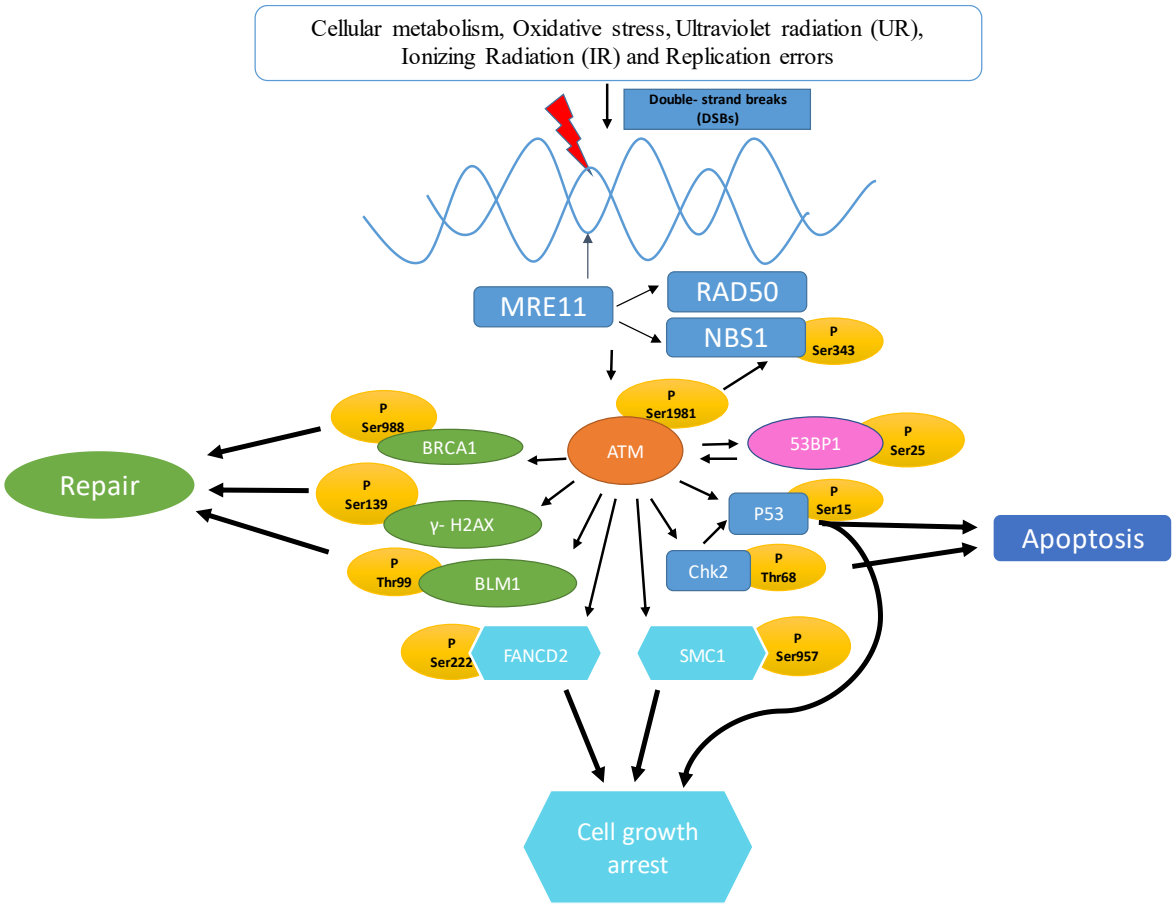

Figure 7. **ATM kinase pathway.** When the cells are exposed to damaging agents, for example, cellular metabolism, oxidative stress, UR, IR and replication errors, DSBs are originated. The DSBs are sensed by MRN complex. Mre11 binds to Nbs1, DNA and Rad50 and ATM phosphorylates Nbs1 at Ser343. MRN complex and Nbs1 are vital to full activation of ATM. The ATM kinase is auto phosphorylated at Ser1981 and consequently its inactive dimer is converted into an active monomeric form in response do DSBs. The ATM kinase phosphorylates several downstream subtracts, namely BRAC1, 53BP1, γ-H2AX, p53, CHK2, FANCD2, SMC1 and BLM1. 53BP1 sustains the DNA damage signaling through ATM activation. The BRAC1, γ-H2AX and BLM1 are responsible for DSBs repair, p53 and Chk2 leads to apoptosis, while FANCD2, SMC1 and p53 activate cell growth arrest. Adapted from[57,62].

1.4 Telomeres

1.4.1 Biology of telomeres

The telomeres are specialized DNA structures constituted by TTAGGG repeat sequences located at the ends of chromosomes[67,68]. Telomeres protect the chromosomal ends from fusion and degradation. Furthermore, they prevent the chromosomes from being accidently recognized as sites of DNA damage by the DNA damage-repair system. Therefore

the telomeres serve as protective caps of chromosomes and they are crucial for the maintenance of genome integrity[68,69].

Structurally, the telomeres of mammalian cells are constituted by telomere DNA, containing double-stranded tandem repeats of TTAGGG followed by terminal 3' G-rich single-stranded overhangs. Telomere DNA adopt T-loop structure when the telomere end folds back on itself and 3' G strand overhang invade into the double-stranded DNA (dsDNA), called D-loop[70] (Figure 8).

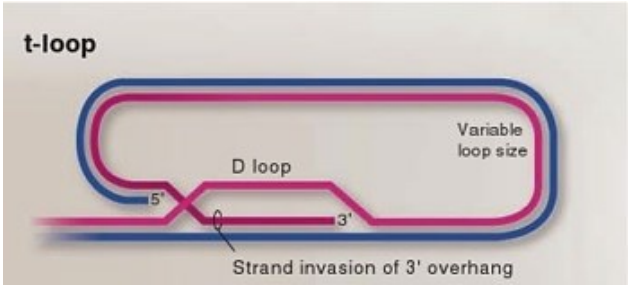

Figure 8. **Structure of mammalian telomeres.** The telomeres are DNA structures constituted by a set of repetitive nucleotides sequences (TTAGGG). Structurally, the telomeres are composed by: i) double-stranded tandem repeats of TTAGGG, ii) 3' G-rich single-stranded overhang, iii) T-loop and iv) D-loop. Adapted from[75].

The telomeres homeostasis is essential to genome stability, cell survival and growth[71]. At each cell division the telomeres lose 30-150 base pairs[72]. The telomerase, a ribonucleoprotein complex, is responsible for maintaining the length of telomeres, preserving healthy cell function and long-term immune function[67,72]. This complex is composed by RNA and proteins components: two copies of telomerase reverse transcriptase (TERT), two copies of its integral RNA template (TERC) and dyskerin protein that binds to TERC and TERT increasing the stability of this complex[69,73] (Figure 9). The TERT is required for the synthesis of new telomeric DNA repeats while the TERC serves as template for syntheses of telomeric DNA[72,74].

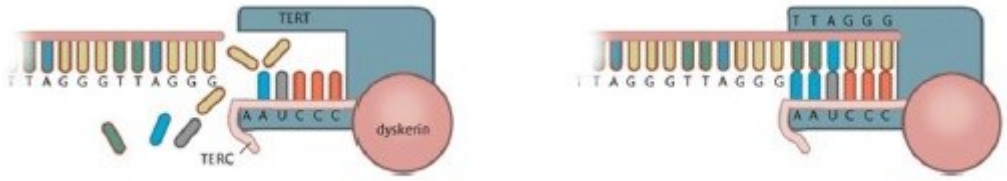

Figure 9. **Structure of telomerase complex.** The telomerase is a ribonucleoprotein complex responsible to maintain and preserves healthy cell function and long-term immune function by maintaining the length of telomeres. This complex is constituted by: i) two copies of telomerase reverse transcriptase (TERT), a fundamental structure for the syntheses of new telomeric DNA repeats ii) two copies of its integral RNA template (TERC), a structure that serves as template for telomeric DNA syntheses and iii) dyskerin protein, a protein that binds to TERT and TERC and increases the stability of this complex. Reproduced from[69].

The shelterin complex is a complex comprised by six proteins, which is crucial for both the maintenance of telomere structure and its signaling functions telomeres, namely Telomeric repeat binding factor 1 (TRF1), TRF2, RAP1, TRF1 interacting nuclear factor 2 (TIN2), tripeptidyl peptidase 1 (TPP1) and protection of telomeres 1 (POT1). TRF1 and TRF2 bind directly to the TTAGGG sequences in double-stranded segment of telomeric DNA[72,75] (Figure 10). POT1 binds directly to the same sequences in single-stranded form (single-stranded DNA (ssDNA)), and it is crucial to the formation of the D-loop when it binds to the 3' overhang and interacts with TPP1[67,72,75] (Figure 9). Rap1, also known as TRF2IP, interacts directly with TRF2 (Figure 10). TIN2 has important complex interactions with TRF1, TRF2 and TPP1[69] (Figure 10). Finally, TIN2 and TPP1 are key components that mediate the activity of the shelterin complex [76].

TRF1 and TRF2 are different elements regarding their function in the shelterin complex. TRF1 has a crucial role telomeres length, while TRF2 prevents the telomere ends from being recognized as DSBs and it is involved in T-loop formation[77]. Regarding shelterin complex proteins, a detailed description of TRF2 and RAP1 is available below, given their importance for this thesis in particular.

Figure 10. **The Shelterin complex.** The mammalian telomeres are composed by a protein complex that regulates the structure of telomeres and protects the chromosome from enzymatic attack, the Shelterin complex. This complex is constituted by six proteins: i) TRF1 that binds to the TTAGGG sequences in double-stranded segments of telomeric DNA and regulates the length of telomeres; ii) TRF2 that also binds to the TTAGGG sequences in double-stranded segment of telomeric DNA, regulates the T-loop formation and protects the telomeres ends from being mistaken as broken DNA; iii) RAP1 also known to TRF2IP that forms a complex with TRF2; iv) TIN2 that stabilizes interactions between TRF1, TRF2 and TPP1; v) POT1 that binds to the TTAGGG sequences in single-stranded form and to TPP1 in order to form the D-loop; vi) TPP1 forms an important complex that allow cells to distinguish telomeres from sites of DNA damage with the TIN2 and RAP1. *Adapted from*[75].

1.4.1.1 TRF2

TRF2 is a protein encoded by the *TERF2* gene and it is responsible for preventing mammalian telomeres from activating DNA damage checkpoints and regulates T-loop formation, as previously mentioned[76]. TRF2 is an ubiquitous protein that is present at more than 100 copies per chromosome end and it is essential for protection of all chromosomes in all steps of cell cycle[78]. Structurally, the TRF2 is composed by four domains: a C-terminal Myb Domain that binds to double-stranded telomeric DNA (TTAGGG); a flexible Hinge domain that is involved in protein-protein interactions; a TRFH domain necessary for homodimerization and a divergent N-terminal domain, which is rich in basic residues (basic domain) (Figure 11). The TRFH domain is required to prevent the first steps of the DNA damage response pathway. The Hinge domain promotes the interaction between TRF2 and two members of shelterin complex involved at the protection of end chromosomes, namely TIN2 and Rap1[79].

Figure 11. **Structure of TRF2 protein.** TRF2 is composed of four domains: i) a C-terminal Myb Domain that binds to double-stranded telomeric DNA (TTAGGG); ii) a flexible Hinge domain that is involved in protein-protein interactions; iii) a TRFH domain necessary for homodimerization and iv) a divergent N-terminal domain rich in basic residues (basic domain). Adapted from[79].

1.4.1.2 RAP1

RAP1 is a protein that belongs to the shelterin complex, known to stabilize the interaction with TRF2[77]. Recently, it was demonstrate that RAP1 binds to TTAGGG telomeric repeats through its interaction with TRF2 and also binds (directly) to chromosome arms where it establishes a vital function, regulation of gene expression[80]. Structurally, RAP1 is constituted by four domains: a N-terminal BRCT domain; a Myb domain; a coiled-coil domain and a C-terminal TRF2-binding RAP1 C-terminal (RCT) domain (Figure 13). The RCT domain binds to the RBM (RAP1 binding motif) domain of TRF2 forming a multifunctional complex, called RAP1/TRF2 complex[81]. The N-terminal BRCT domain binds to a phosphorylated target protein when dimerized in the shelterin complex, while the C- terminal serves to anchor the protein in shelterin complex[82].

Figure 12 **RAP1 proteins structure**. RAP1 protein is constituted by four domains: i) N-terminal BRCT domain that binds a phosphorylated target protein when dimerized in the Shelterin complex; ii) Myb domain; iii) coiled- coil domain and iv) RCT domain that binds to RBM domain of TRF2 protein. Adapted from[81].

1.4.1.3 Expression of TRF2/RAP1 proteins upon DNA damage

Recently, some proteins that play important roles in DNA repair have also been associated to telomere maintenance. Members of PIKKs family, such as ATM and DNA-PKcs are involved in the maintenance of genomic stability via DNA repair pathways. These members appear also appear to be involved in telomere maintenance[83]. The mechanisms of communication between these two major cellular processes have intensified[84]. The telomeres act as protective caps to prevent chromosome ends from being recognized as DSBs, as previously reported. When telomeres become dysfunctional, chromosomes ends activate a DNA damage response mediated by ATM[84,85]. When ATM kinase is activated, the chromosome ends become associated with DNA damage response factors, such as 53BP1, γ-H2AX, and the MRN complex[83]. The mechanism by which telomeres prevent these events has been investigated[85]. TRF2 inhibits autophosphorylation of ATM kinase on Ser 1981 at telomeres and it is required to prevent mammalian telomeres from activating DNA damage checkpoints[83].

RAP1 forms a multifunctional complex with TRF2. This complex stabilizes interactions with a set of key proteins in the DNA damage pathway, namely ATM, MRN complex, Ku, DNA-PKcs, WRN (Werner syndrome protein), BLM and cooperates in functions of DNA repair[77,86]. TRF2 associates the telomeres to proteins involved in DSB repair. TRF2 has also been associated with a new non-telomeric function, namely in DNA repair response mechanisms. This protein has an intrinsic ability to interact with DSBs and, in response to DNA damage, it is phosphorylated by ATM migrating rapidly to specific sites of DNA damage caused by DSBs (laser microbeam irradiation)[84,87]. The phosphorylated form of TRF2 is involved in telomere DNA repair by recruitment of additional DNA repair proteins to damaged telomeric DNA, playing a crucial role in DNA damage signaling responses. However, the exact role of TRF2 during DNA damage response remains to be determined[84].

Objectives

2. Objectives

LAP1 is a type II transmembrane protein encoded by the *TOR1AIP1* gene and it is located at the INM. Several LAP1 functions have been described due to the identification of its binding partners. These binding partners include lamins, torsinA, emerin and PP1, which convey crucial cellular functions to LAP1 itself, namely in nuclear architecture maintenance and chromatin regulation (LAP1: lamins), regulation of torsinA ATPase activity, nuclear envelope localization of torsinA and NE dynamics (LAP1: torsinA), nuclear envelope integrity maintenance and skeletal muscle maintenance (LAP1: emerin), and regulation of cell cycle progression (LAP1: PP1). Furthermore, several novel putative LAP1 interactors are emerging. In fact, recent data from our group allowed the identification of several novel putative LAP1 functionally associated proteins, namely TRF2, RAP1, RIF1, ATM, MAD2L1 and MAD2L1BP. Some of these proteins are involved in DNA damage response and telomere signaling.

Therefore, the main objective of this thesis is to expand the knowledge of LAP1 in the DNA damage response and in cell cycle progression, through the study of two of its putative protein interactors, namely TRF2 and RAP1.

The specific aims of this thesis are:

- To establish TRF2 and RAP1 as novel LAP1 interactors;
- To determine the expression levels of LAP1 and TRF2 during DNA damage induced by Hydrogen Peroxide (H_20_2);
- To evaluate the subcellular distribution of LAP1 and TRF2 during DNA damage;
- To further access the subcellular distribution of LAP1 and TRF2 during cell cycle progression.

Materials and Methods

3. Materials and Methods

3.1 Cell Culture

The SH-SY5Y human neuroblastoma cell line is derived from the cell line SK-N-SH which was extracted from a bone marrow biopsy of a neuroblastoma patient. HeLa cells are an immortalized line cell derived from human cervical carcinoma. SH-SY5Y were maintained in Minimum Essential Media (MEM) supplemented with F-12 nutrient mixtures (Gibco), 10% fetal bovine serum (FBS; Gibco), 1.5 mM L-glutamine and 100 U/mL penicillin and 100 mg/mL streptomycin). HeLa cells were maintained in Dulbeco's Minimum Essential Media (DMEM; Gibco) supplemented with 10% FBS (Gibco) and 1100 U/mL penicillin and 100 mg/mL streptomycin. Culture medium was changed every other day and cells were subcultured when 90-95% confluence was reached. All the cultures were maintained in a 5% CO_2 humidified incubator at 37ºC.

3.2 Antibodies

To detect the proteins analyzed in the experimental procedures of this dissertation several primary antibodies were used, namely anti-LAP1[88], anti-RAP1 (Abcam), anti-TRF2 (Abcam) and anti-γ-H2AX (Millipore). The selection of the secondary antibodies was achieved according to the specific technique used, namely, immunocytochemistry (ICC) and western blot (WB). For WB, the secondary goat antibodies with horseradish peroxidase (HRP) (GE Healthcare) were used to recognize mouse or rabbit primary antibodies. For ICC assays Alexa Fluor 488 goat-anti rabbit and Alexa Fluor 594 anti-mouse (Life Technologies) were used. Tables 1 and 2 summarize the multiple antibodies used and their respective dilutions.

Table 1 **Summary of the primary antibodies used to detect target proteins and specific dilutions used for different assays.** BSA, Bovine Serum Albumin; PBS, Phosphate-buffered saline solution; TBS-T, Tris-buffered saline-Tween; ICC, Immunocytochemistry; WB, Western Blot; Co-IP, Co-Immunoprecipitation.

Primary Antibody	Antibody type	Target	Dilution	Blocking Solution
Anti-LAP1	Rabbit, polyclonal	LAP1	ICC 1:4000	3% BSA/ 1x PBS
			WB 1:20000	3% BSA/1x TBS-T
			Co-IP 0.2 µl per 2500 µg protein	
Anti-RAP1	Mouse, monoclonal (Abcam)	RAP1	WB 1:5000	3% BSA/1x TBS-T
			Co-IP 5µg per mL	
Anti-TRF2	Mouse, monoclonal (Abcam)	TRF2	ICC 1:500	3% BSA/ 1x PBS
			WB 1:2000	3% BSA/1x TBS-T
			Co- IP 2 µg per 10^6 cells	
Anti-γ-H2AX Ser 139	Mouse, monoclonal (Millipore)	γ- H2AX Ser139	ICC 2 µg per mL	3% BSA/ 1x PBS
			WB 1:500	3 % BSA/ 1x TBS-T

Table 2 **Summary of the secondary antibodies used to detect target proteins and specific dilutions used for different assays.** BSA, Bovine Serum Albumin; PBS, Phosphate-buffered saline solution; TBS-T, Tris-buffered saline-Tween; ICC, Immunocytochemistry; WB, Western Blot.

Secondary Antibodies	Antibody type	Dilution	Blocking Solution
Alexa Fluor 488	Goat, anti-rabbit	ICC 1:300	3% BSA/ 1x PBS
Alexa Fluor 594	Goat, anti-mouse	ICC 1:300	3% BSA/ 1x PBS
α-ECL anti-mouse	Goat, anti-mouse	WB 1:5000	3% milk/ 1× TBS-T
α-ECL anti-rabbit	Goat, anti-rabbit	WB 1:5000	3% milk/ 1× TBS-T

3.3 HeLa cells exposure to different concentrations of H_20_2

Oxidative stress induces a variety of different types of DNA damage, including purine and pyrimidine damage, sugar moiety damage, SSBs and DSBs. Hydrogen Peroxide (H_20_2) is one Reactive oxygen species (ROS) involved in many cellular functions, such as development, proliferation and differentiation. This molecule is involved in ATM activation, H2AX phosphorylation and DSBs generation[57,89,90].

To induce DNA damage, HeLa cells were exposure to different concentrations of H_20_2 (Acros Organic). Therefore, cells were plated in 12-well plates (Corning) with a cell density of $1.6x10^5$ cells per well and incubated at 37ºC with 5% CO_2 for 16 hours. Upon this period, cells were incubated with standard medium with deferential H_20_2 concentrations: 20, 40 and 80 µM of H_20_2. In the control condition, no H_20_2 was added. The different H_20_2 concentrations were prepared from a H_20_2 stock solution (10 mM). Cells were incubated with H_20_2 for 0, 6 and 12 hours. At those specific time points HeLa cells were trypsinzed and resuspended in culture medium and the cell viability determined, as described below.

3.4 Cell Viability

HeLa cells growing curve upon H_20_2 treatment, was determined using the trypan blue (TB) exclusion dye method. Trypan blue penetrates the membrane of dead cells which became colored in blue. In living cells the plasma membrane is intact and it is not permeable to TB, remaining uncolored. At all times points, 10 µl of trypan blue (Sigma) were added to 90 µl of cell suspension and counted in duplicate in the hemocytometer. A cell viability curve was calculated based on these values and the data is represented with the mean ± SEM from at least 3 independent experiments performed in duplicate, adding up to 6 experiments in total.

3.5 Measurement of cell death

Apoptotic cells show alterations in nuclear morphology. These alterations can be measured by the assessment of nuclear staining. Healthy cells show diffuse staining of the nucleus unlike the apoptotic cells. The alterations in nuclear morphology of apoptotic cells can be divided in three classes: i) chromatin condensation; ii) nuclear fragmentation and iii) nuclear condensation. The chromatin condensation is characterized by chromatin margination without nuclear condensation, the nuclear fragmentation is characterized by chromatin margination with nuclear condensation and nuclear condensation is characterized by a decreasing of nuclei size without chromatin margination[91] (Figure 13). Measurement of cell death can be assessed by fluorescence microscopy using 4', 6-diamidino-2-phenylindole (DAPI).

To measure cell death, HeLa cells were plated in 12-well plates with a seeding density of $1.6x10^5$ cells per well and incubated at 37ºC with 5% CO_2 for 16 hours. After 16 hours, cells were incubated with different concentrations of H_20_2 (20, 40 and 80 μM of H_20_2). The control condition with no addition H_20_2 was also performed. In different times points (0, 6 and 12 hours), the cells were washed with 1x PBS and then fixed with 4% paraformaldehyde (PFA) for 20 minutes. After fixation, the cells were washed three times with 1mL of 1x PBS. Then, the samples were mounted on a microscope slide with DAPI-containing VECTASHIELD® Mounting media (Vector Laboratories). The microscope slides were visualized in a fluorescent microscope, using the objective 20x in Olympus IX-81 (Olympus, Optical Co. GmbH) motorized inverted microscope equipped with a PlanApo/ 1.40 oil immersion objective lens. Photographs were obtained with a digital CCD monochrome camera F-view II (Soft Imaging System). The percentage of apoptotic cells was calculated in each condition.

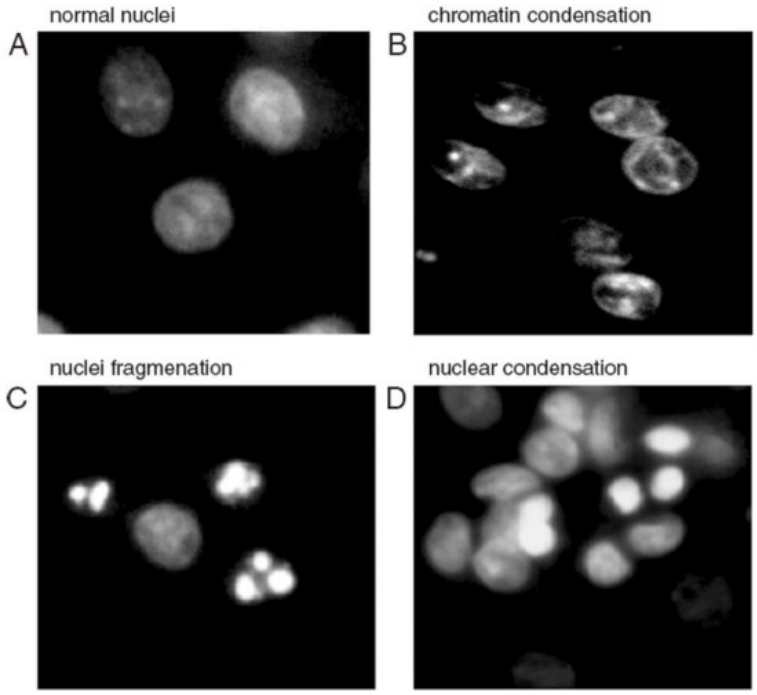

Figure 13. **Representative DAPI staining of healthy and apoptotic nucleus.** A) Staining of normal nuclei, B) Chromatin condensation, C) Nuclear fragmentation and D) nuclear condensation. Reproduced from[91].

3.6 Proteomic Assays

3.6.1 Cell collection and protein quantification

Cell's conditioned media was centrifuged at 1000 rpm for 3 min, washed with 1x PBS and newly centrifuged. Following, the cells were resuspended in 100 µl (12 well) of 1% SDS for WB. The cell lysates were boiled at 90ºC for 10 min, sonicated for 5 secs and stored at -20ºC.

To quantify the total protein content of cell lysates the Pierce's bicinchoninic acid (BCA) protein assay kit (Thermo Scientific) was used. This assay is a detergent-compatible formulation based on BCA for calorimetric detection and quantification of total protein. The method is based in the reduction of Cu^{2+} to Cu^{+} by protein in an alkaline medium. Cu^{+} interacts with bicinchoninic acid which results in the formation of an intense purple-colored reaction product, a water-soluble complex that can be measured at 562 nm with increasing protein concentrations over a working range of 0.02-2 µg/µL. The total reduction of Cu^{2+} to Cu^{+} is equivalent to protein concentration which is determined by comparison to standard samples, these were prepared through of bovine serum albumin (BSA)[92] as described in table 3.

Table 3. **Standards preparation**. BSA, Bovine Serum Albumin.

Standards	BSA (µL)	Extraction Buffer (µL)	Protein mass (µg)	Concentration (µg/ µL)
P0	0	25	0	0
P1	1	24	2	0.08
P2	2	23	4	0.16
P3	5	20	10	0.4
P4	10	15	20	0.8
P5	20	5	40	1.6

3.6.2 SDS-PAGE

The samples were separated on a sodium dodecyl sulphate-polyacrylamide gel electrophoresis (SDS-PAGE), a denaturing gel that allows the separation of proteins according to their molecular weight, followed by electrotransference of the immobilized proteins into a nitrocellulose membrane. The membranes will be further used for the immunological detection of the proteins of interest using specific antibodies. To analyze the co-immunoprecipitation experiments a 7.5% polyacrylamide gel was used (since TRF2, RAP1, LAP1B and LAP1C have molecular weights around 50 kDa and 75 kDa). To analyze the LAP1, γ-H2AX and TRF2 expression upon H_20_2 treatment, a gradient gel (5-20%) was used.

Prior to loading, the samples were prepared by the addition 1x loading buffer (LB), boiled for 10 minutes and spinned down. To identify the molecular weight a Precision plus Protein ™ Dual Colour Standards (Bio Rad) marker was used. Proteins were separated using an electrical current to the gel (90 mA) for 3/4 hours.

3.6.3 Immunoblotting

In our experimental system, after electrophoresis, proteins were transferred to nitrocellulose membranes (0.2 μm pore size; Whatman) for 18 hours at 200 mA and then visualized with specific antibodies. The nitrocellulose membranes were hydrated with 1× TBS for 10 minutes and incubated with a Ponceau S Solution (Sigma Aldrich) for 5 min, followed by a wash with deionized water to make the protein bands clearly visible. The membranes were scanned in a GS-800 calibrated imaging densitometer (Bio-Rad) and then washed with 1x TBS-T for complete removal of the Ponceau S staining. The Ponceau S staining is applied to assess successful transference of proteins to the membrane.

The nitrocellulose membranes were blocked to prevent non-specific binding of primary antibodies[93] with 5% BSA/1x TBS-T for 3/4 hours and further incubated with primary antibodies. The incubations with anti-TRF2 (mouse), anti-RAP1 (mouse) and anti-γ-H2AX (mouse) were performed overnight. The incubations with the anti-LAP1 (rabbit) were carried out for 4 hours. After the incubation with primary antibodies, the nitrocellulose membranes were incubated with anti-mouse/rabbit horseradish peroxidase conjugated secondary antibodies for 2 hours. After 3 washes with 1x TBS-T the membranes were incubated for 1 min with enhanced chemiluminescence (ECL) detection kit, for 5 minutes with Luminata™ Crescendo Western HRP Substrate (Millipore) or for 4 minutes with ECL™ Select WB detection reagent (GE Healthcare) in ChemiDoc™ Touch Imaging System (Bio-Rad). ECL™ is a light non-radioactive method to detect immobilized antigens that are directly or indirectly conjugated with horseradish peroxidase (HRP)-labelled antibodies.

3.6.4 Immunocytochemistry assay

The immunocytochemistry (ICC) is a technique that through protein-antibody interactions allows the visualization of the location of a specify protein and their subcellular localization[94].

Initially, the cells were washed with 1x PBS and then fixed with 4% paraformaldehyde (PFA) for 20 minutes to stabilize and preserve cells as close to life-like as possible. Afterwards, the cells were washed trice with 1x PBS and permeabilized with the addition of a detergent, 0.2 % Triton in PBS for 10 minutes, which solubilizes cellular membranes without destroying protein-protein interactions and allows that the antibodies

and other probes penetrate inside. Then, the cells were blocked with 3% BSA/1x PBS for 1 hour to block non-specific binding sites.

Following blocking, the samples were incubated with the proper specific primary antibody and fluorochrome-labeled secondary antibodies diluted, both in 1x PBS/ 3% BSA, for 2 and 1 hours respectively, as described in table 1 and 2. The cells were washed thrice with 1x PBS following permeabilization, between antibody incubation periods and after incubation with the secondary antibodies. Then, the samples were mounted on a microscope slide with DAPI-containing VECTASHIELD® Mounting media (Vector Laboratories). The microscope slides were visualized in a fluorescent microscope, using the Olympus IX-81 (Olympus, Optical Co. GmbH) motorized inverted microscope equipped with a PlanApo/ 1.40 oil immersion objective lens. Photographs were obtained with a digital CCD monochrome camera F-view II (Soft Imaging System).

Table 4. **Summary of the excitation and emission wavelengths of the secondary antibodies**.

Fluorophores	Excitation maximum (nm)	Emission maximum (nm)	Observed color
Alexa Fluor 488	495	519	Green
Alexa Fluor 594	590	617	Red

3.6.5 Co-immunoprecipitation assay

The SH-SY5Y cells were washed with cold 1x PBS and then gently scrapped off the culture plate with in 1 mL of CHAPS lysis buffer (50 mM Tris-HCl pH=8, 120 mM NaCl, 4% CHAPS) that contains protease inhibitors (1 mM PMSF, 10 mM Benzamidine, 2 µM Leupeptin, 1.5 µM Aprotinin, 5 µM Pepstatin A). Then, the lysates were mass-normalized using BCA assay and were precleared with 10 µl Protein G Dynabeads for 1 hour at 4°C with agitation.

In a new microtube, 40 µl of Protein G Dynabeads were added to 400 µl of washing solution (3% BSA in PBS) containing the primary antibody, respectively LAP1, TRF2 or RAP1 at respective dilutions, as described in table 1 for 1 hour at 4ºC with agitation. The Protein G Dynabeads bind to the Fc region of primary antibodies, the immune complex is precipitated on a beaded support to which an antibody-binding protein is immobilized.

After 1 hour, the samples were added to the microtube that contains the primary antibody and Protein G Dynabeads and incubated overnight at 4ºC with agitation. Then, the supernatant was removed and the beads were washed with 400 µl of 1x PBS for 10 min at 4º C with agitation. The microtube is placed on a magnet, where the beads migrate to the side of the tube facing the magnet and allowed for easy removal of the supernatant. After the last wash, the supernatant was fully discarded and the beads were resuspended in 100 µl of 1x LB and boiled for 10 min at 90º C for disruption of the Protein G Dynabeads from the antibody protein complexes. Finally, the Protein G Dynabeads were magnetically removed and the immunoprecipitates were resolved in a 7.5% SDS-PAGE followed by immunoblotting.

3.7 Quantification and statistical analysis

Ponceau-stained membranes were scanned using GS-800 imaging densitometer (Bio-Rad) and protein bands were quantified through the Image Lab™ software (Bio-Rad). This software quantifies band intensity and correlates it to proteins levels. All the data was corrected for the loading control (Ponceau-S) and the fold increase was calculated in relation to the control (0 µM) and expressed as mean ± SEM. The statistical analysis was performed using one-way ANOVA and t-test with the GraphPad prism 6 software. The one-way ANOVA test was performed within each concentration of H_20_2 and time point, followed by the Dunnets test (for comparison of data with control values)[95]. The t-test was performed to compare the means between two groups (control and 80µM of H_20_2) at 12 hours[95].

Results

4. Results

4.1 Identification of TRF2 as novel LAP1 interactor by Co-Immunoprecipitation

Protein-protein interactions are involved in all cellular processes. When a protein-protein interaction is identified, it is essential to validate the interaction and establish the physiological function in a biological system. Co-immunoprecipitation is a technique crucial to validate interactions between proteins and it is based on the formation of antigen-antibody complexes[96]. A recent study from our group reported that LAP1 can stabilize interactions with two proteins of shelterin complex, namely TRF2 and RAP1[45]. To identify TRF2 and RAP1 as novel LAP1 interactors, co-immunoprecipitation assays were performed in SH-SY5Y cells. Initially, different acrylamide percentages were tested to separate the gel around 75-50 kDa and to avoid the intense signal from the immunoglobulin heavy chains (50 kDa) which might overlap with the LAP1C (56 kDa) band signal. SH-SY5Y cells were immunoprecipitated with anti-LAP1 antibody, anti-TRF2 and anti-RAP1 antibodies (Figure 14-16). Cells lysates and co-immunoprecipitates were separated by 7.5% SDS-PAGE and then transferred to a nitrocellulose membranes. Then, these nitrocellulose membranes were immunoblotted with anti-LAP1, anti-TRF2 and anti-RAP1 antibodies and developed by ECL (Figure 14-16).

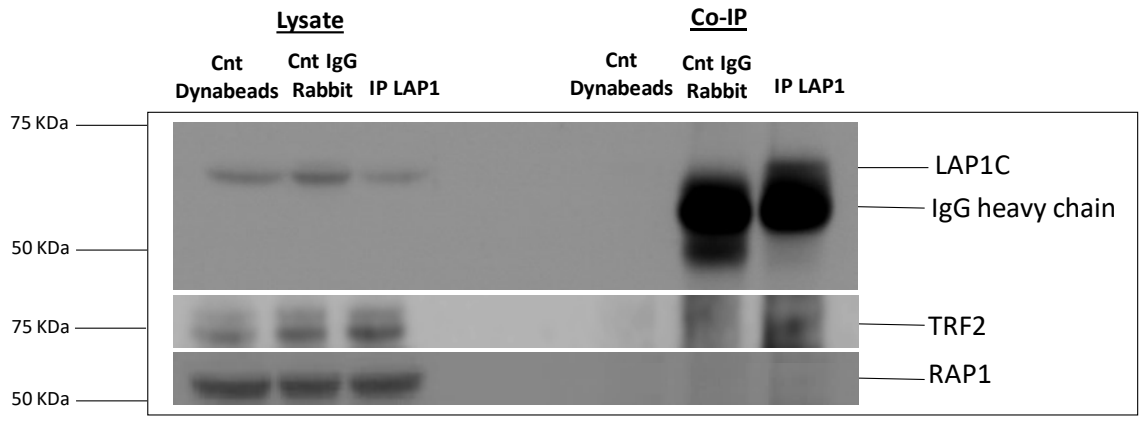

Figure 14. **Validation of LAP1 interaction with TRF2 and RAP1 by Co-Immunoprecipitation.** Immunoblot analysis of SH-SY5Y cells immunoprecipated with anti-LAP1 and immunoblotted with anti-LAP1, anti-TRF2 and anti-RAP1. Dynabeads (Cnt Dynabeads) alone and Dynabeads plus Rabbit IgG (Cnt IgG Rb) were used as negative controls.

As shown in figure 14, LAP1 was efficiently immunoprecipitated using the anti-LAP1 antibody, since LAP1C isoform was only detected in the immunoprecipitation condition. The TRF2 antibody detects two bands around 65 and 69 kDa, these polypeptides share highly homologous motifs and are collectively termed TRF2[97,98]. Therefore, using the anti-TRF2 antibody we were able to detect two bands of 65 and 69 kDa indicating that TRF2 was successfully co-immunoprecipitated with LAP1 and the two proteins interact (Figure 14). However, RAP1 was not co-immunoprecipitated with LAP1 antibody (Figure 14). The immunoprecipitations were also carried out using both TRF2 and RAP1 antibodies. The results of co-immunoprecipitation using the TRF2 antibody are presented in Figure 15.

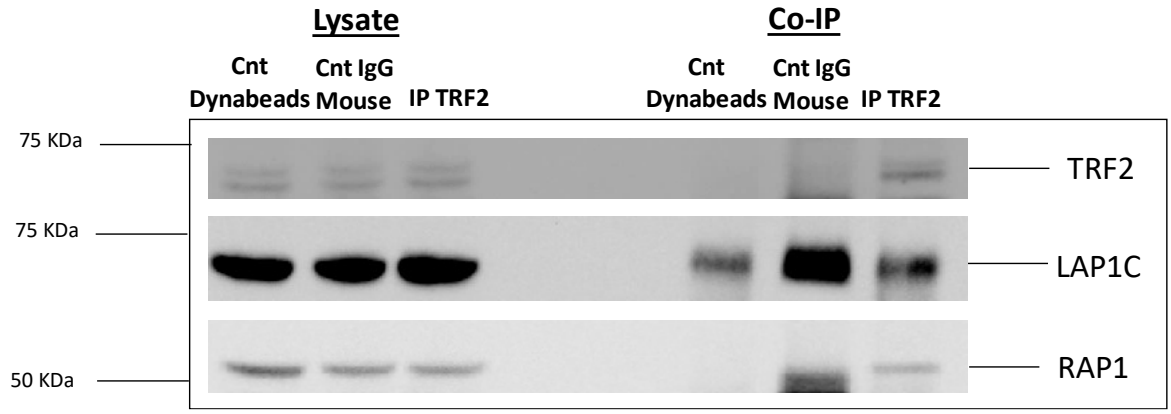

Figure 15. **Validation of TRF2 interaction with LAP1 and RAP1 by Co-Immunoprecipitation.** Immunoblot analysis of SH-SY5Y cells immunoprecipated with anti-TRF2 and immunoblotted with anti-TRF2, anti-LAP1 and anti-RAP1. Dynabeads (Cnt Dynabeads) and Dynabeads plus Mouse IgG (Cnt IgG Ms) were used as negative controls.

As shown in figure 15, TRF2 was successfully immunoprecipitated, since TRF2 was immunoprecipitated only when the TRF2 antibody was used and not with the negative controls (Figure 15). Further, LAP1C was also detected when the co-immunoprecipitation performed with TRF2 antibody (Figure 15). However, LAP1C seems to bind non-specifically to negative controls, namely Dynabeads and Dynabeads plus Mouse IgG (Figure 15). In addition, when co-immunoprecipitation of TRF2 was immunoblotted with anti-RAP1 antibody, it was showed that TRF2 interacts with Rap1, as previously reported (Figure 15)[81]. The results of co-immunoprecipitation using the Rap1 antibody are presented in Figure 16.

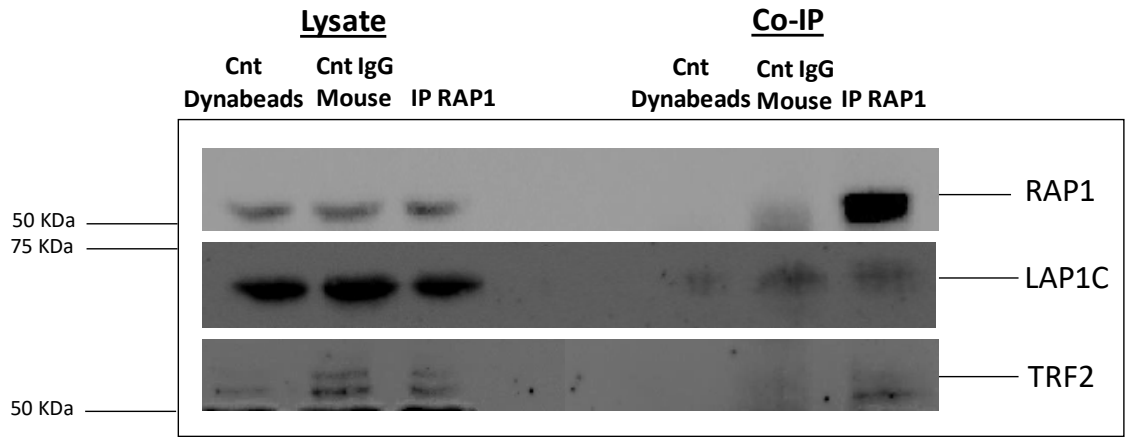

Figure 16. **Validation of RAP1 interaction with TRF2 and LAP1 by Co-Immunoprecipitation.** Immunoblot analysis of SH-SY5Y cells immunoprecipated with anti-RAP1 and immunoblotted with anti-RAP1, anti-LAP1 and anti-TRF2. Dynabeads (Cnt Dynabeads) and Dynabeads plus Mouse IgG (Cnt IgG Ms) were used as negative controls.

RAP1 was successfully immunoprecipitated, since RAP1 was immunoprecipitated only when RAP1 antibody was used and not with negative controls (Figure 16). The LAP1C also was detected in co-immunoprecipitation of RAP1 (Figure 16), however, as referred previously, LAP1 seems to bind non-specifically to negative controls, namely Dynabeads and Dynabeads plus Mouse IgG (Figure 16). In addition, RAP1 also interacts with TRF2, as indicated by our previous results (Figure 15) and as described in literature[81].

4.2 Identification of TRF2 as novel LAP1 interactor by liquid chromatography-mass spectrometry

A different approach based on HPLC-MS technique (High performance liquid chromatography-mass spectrometry) was used in order to confirm that both TRF2 and RAP1 are in fact novel LAP1 binding proteins. SH-SY5Y cells were incubated with different concentrations of OA (Okadaic Acid), namely 0, 0.25 and 500 nM. The 0.25 nM concentration of OA inhibits PP2A (Protein phosphatase 2A) and 500 nM of OA inhibits both PP2A and PP1[37]. In order to identify the enrichment of TRF2 and RAP1 peptides in each condition, cells were co-immunoprecipitated using the LAP1 primary antibody. The samples were loaded on a 10 % SDS-PAGE followed by Coomassie blue colloidal staining. The bands that corresponds to LAP1C (56 kDa) and LAP1B (68 kDa) were excised. Following careful excision, the bands were tryptically digested and analyzed in a Nano-

HPLC system online coupled to a Q Exactive mass spectrometer (Thermo Fisher Scientific, Germany) (Table 5). Of note, this experience was performed by a previous member of our group, Mariana Santos, to validate new isoform of LAP1 (LAP1C). The results were further analyzed in order to detect peptides corresponding to TRF2 and RAP1 peptides[41].

Table 5. **TRF2 and RAP1 peptides identified by HPLC-MS analysis.** The SH-SY5Y cells were treated with different concentrations of OA (Okadaic Acid) and co-immunoprecipitated with LAP1 antibody. These were loaded in 10% SDS-PAGE and stained with Coomassie blue colloidal staining. The bands corresponding to LAP1B (68 kDa) and LAP1C (56 kDa) were excised and analyzed by HPLC- MS. The number of peptides of TRF2 and RAP1 are identified in each condition.

Peptides		**LAP1B (68 kDa) +LAP1C (56 kDa)**		
		IP OA 0nM	**IP OA 0.25 Nm**	**IP OA 500 nM**
TRF2	QPAPGPVEKPPREPAR			
	TLSGAQDSEAAFAK			
	TEFTLTEAVVESSR			
	DLVLPTQALPASPALK			
	WTVEESEWVK			
	DIMQALLVRPLGK			
	NLAHPVIQNFSYETFQQK			
	NDLLNIIR			
	FYFHEALR			
	NDLLNIIR			X
	FLESHLDDAEPYLLTMAK			
	DLVLPTQALPASPALK			X
RAP1	SSLTQHSWQSLKDR			
	SPSSVTGNALWK			
	FNLDLSTVTQAFLK			
	IAFTDADDVAILTYVK			
	NSGELEATSAFLASGQR			
	EIGILTTNK			
	KPIDYTILDDIGHGVK			
	IIAPANLERPVR			
	TLEPVRPPVVPNDYVPSPTR			
	SSLTQHSWQSLKDR			
Number of peptides		0	0	2

Overall, for all conditions analyzed, only two TRF2 peptides were identified when LAP1 was immunoprecipitated, namely with 500 nM of OA (Table 5). Of note is that, at this condition both PP1 and PP2A were inhibited. Therefore, it seems that TRF2 interacts with LAP1 when it reaches its phosphorylation stage (inhibition of PP1 and PP2A). RAP1 peptides were not found in any of the co-immunoprecipitation conditions.

4.3 Potential role of LAP1:TRF2 during DNA damage

4.3.1 Optimization of HeLa cells growth curve upon H_20_2 exposure

LAP1 is a transmembrane protein of the NE which is phosphorylated by ATM during mitosis[40]. ATM is a kinase involved in DNA damage response and it is activated by oxidative stress induced by Hydrogen Peroxide (H_20_2)[57,90]. In telomeres, TRF2 interacts with a set of key proteins involved in the DNA damage response, namely ATM, MRN complex, Ku, WRN and BLM, together cooperating in functions of DNA repair[87]. In this study, TRF2 was identified as a novel LAP1 interactor. TRF2 protects mammalian telomeres from the activation of DNA damage checkpoints[83] and it interacts with DSBs in response to DNA damage induced by laser microbeam irradiation[84,87]. To understand the LAP1 physiological roles it is important the identification of novel LAP1 binding proteins and their cellular functions. Therefore, one of the aims of this thesis was investigate the role of LAP1 and TRF2 during DNA damage induced by oxidative stress. To induce DNA damage, several H_20_2 concentrations were tested in order to induce DNA damage. HeLa cells were seeded with a cell density of 0.5×10^5 cells per well and the plates cultured for 16 hours at 37ºC in a humidified chamber with 5% CO_2. The cells were treated with different concentrations of H_20_2, namely 0, 100, 200, 400, 800 and 1000 µM and collected at several specific time points (0, 6, 12 and 24 hours). The cell viability was measured using the Trypan blue assay (Figure 17). The concentrations of H_20_2 and the times points were chosen according to a published study[65].

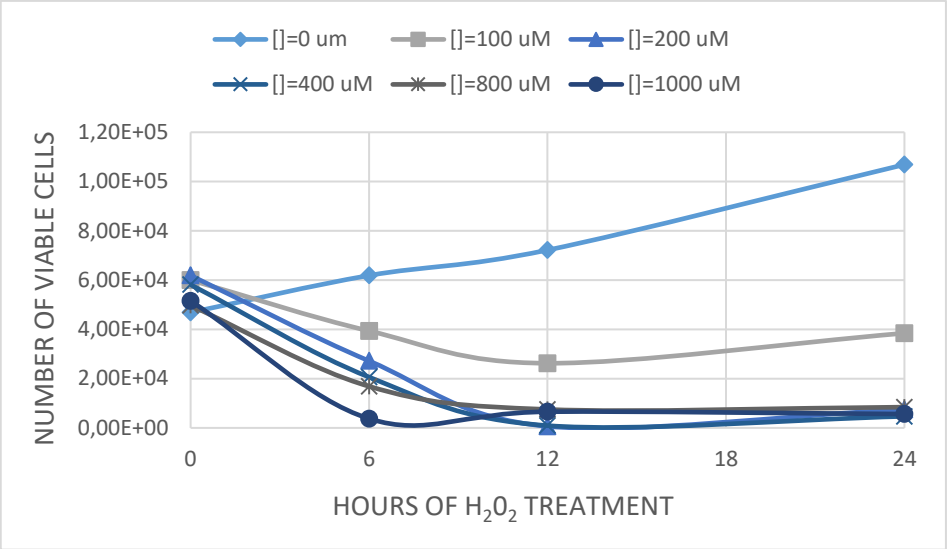

Figure 17. **Effects of H_2O_2 on the cell growth of HeLa cells.** Cells were treated with the indicated concentrations of H_2O_2 for 0h, 6h, 12h and 24 hours.

All concentrations of H_2O_2 tested lead to a reduction of cell viability, except in the untreated control (0 µM). At 100 µM of H_2O_2, there was a reduction in the number of viable cells until the 12 hours' time-point, and remain constant there after (Figure 17). Concentrations between 200 and 1000 µM of H_2O_2 significantly induce cell death and growth inhibition (Figure 17). Therefore, we decided to test lower concentrations of H_2O_2. The experiment above was repeated and DNA damage was induced with novel concentrations of H_2O_2, namely 0, 10, 20, 40, 80 and 160 µM. In each time point (0, 6, 12, 18 and 24 hours) cell viability was measured with the Trypan blue assay.

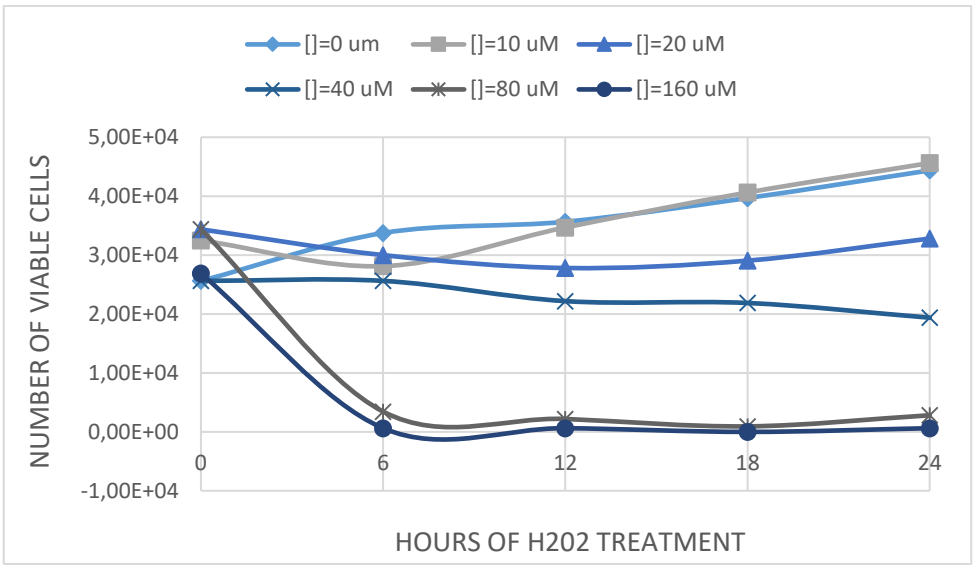

Figure 18. **Effects of H_2O_2 on the cell growth of HeLa cells.** Cells were treated with the indicated concentrations of H_2O_2 for 0, 6, 12, 18 and 24 hours.

Apparently, no reduction of cell viability with the lowest H_20_2 (10 µM) concentration was observed (Figure 18). With 20 µM of H_20_2, the number of viable cells decreases until the 12 hours' time point but afterwards the cells seem to recuperate (Figure 18). At 40 µM, the cell curve maintains a linear behavior, whereas 80 and 100 µM of H_20_2 lead to a reduction of the viable cell number count until the 24 hours' time point (Figure 18). After these analysis, we verified that lower concentrations induce a limited reduction in the number of viable cells but higher concentrations lead to a dramatic reduction in the number of viable cells at all times points. After analysis of these results, we decided that the ideal H_20_2 concentrations for subsequent studies are from 0, 20, 40 and 80 µM. The incubation periods selected were 0, 6 and 12 hours.

4.3.2 Effects of H_2O_2 on the cell growth in HeLa cells

To evaluate the physiological role of LAP1 and TRF2 during DNA damage induced by H_20_2, the number of seeding cells was optimized, after optimization of H_20_2 concentrations and respective times points. We also decide to increase the number of cells seeded per well, since we consider that with the concentration of 0.5×10^5 cells per well, the cells were not with the adequate confluency upon 16 hours. 12-well plates were seeded with 1.6×10^5 cells and cultured for 16 hours at 37ºC in a humidified 5% CO_2 chamber. After 16 hours, different concentrations of H_20_2 (0, 20, 40 and 80 µM) were added to the cells. The cells were collected at the different times points and the number of viable cells was counted through the Trypan blue assay. The cell viability results were similar to the previous experiment (Figure 19), and therefore we decide to work with this concentration in future experiments.

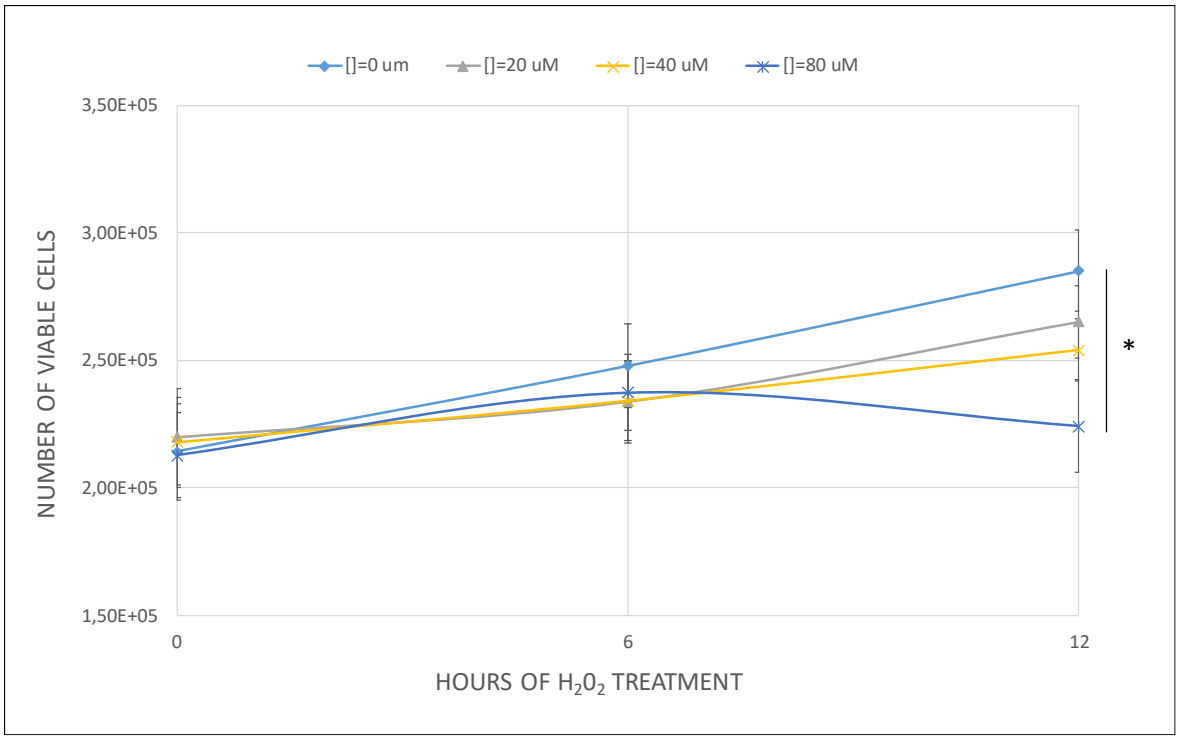

Figure 19. **Effects of H_2O_2 on the cell growth of HeLa cells.** Cells were treated with the indicated concentrations of H_20_2 for 0, 6 and 12 hours. Data are presented as mean ± SEM of at least six independent experiments (n=6). *p< 0.05 statistic symbol: * for comparisons between 0µM and 80µM of H_20_2 at 12 hours, by using one-way ANOVA followed by the Dunnets test.

The number of viable cells in all concentrations tested apparently increase at the 6 hours' time point (Figure 19). The number of viable cells increases at 12 hours' time point with both 20 µM and 40 µM of H_20_2 concentrations, but the number of viable cells with the highest H_20_2 concentration (80 µM) significantly decrease at 12 hours' time point ($p< 0.05$, by one-way ANOVA followed by the Dunnets test) (Figure 19 and Appendix 1A). These results showed an average of six experiments (n=6).

4.3.3 Percentage of apoptotic cells

As visualized in the previous experiments, the number of viable cells varies along the curve according the H_20_2 concentration (Figure 19). To assess the effect of H_20_2 in the apoptotic mechanism we decide to measure the percentage of apoptotic nucleus induced by different H_20_2 concentrations. HeLa cells were seeded and incubated at 37ºC with 5% CO_2 for 16 hours. After 16 hours, cells were incubated with different concentrations of H_20_2 (20, 40 and 80 µM of H_20_2). The control condition has no addition of H_20_2. In each time point (0, 6 and 12 hours) the cells were fixed and the samples were mounted on a microscope slide with DAPI-containing VECTASHIELD® Mounting media. The number of apoptotic nucleus was counted in each condition (Figure 20-22).

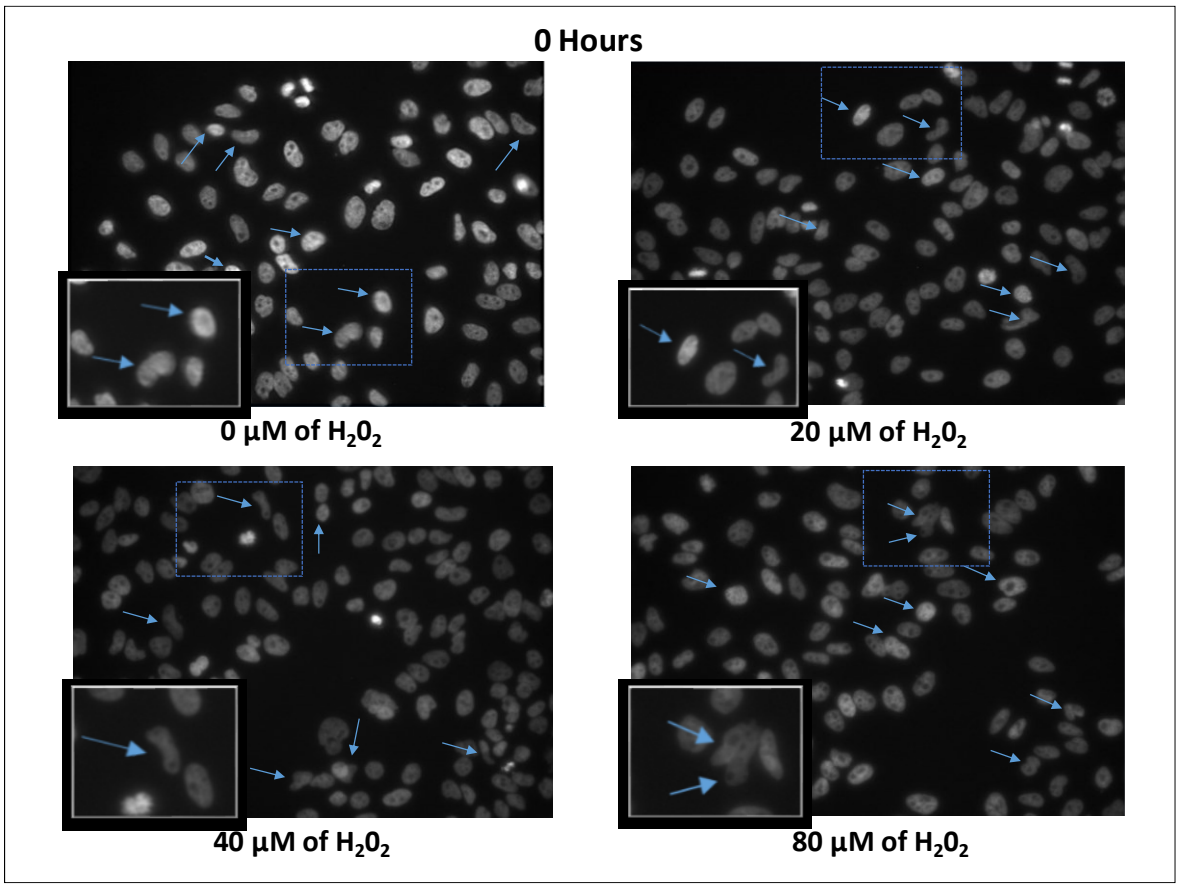

Figure 20. **Representative DAPI staining of apoptotic nucleus in different concentrations of H_20_2 at 0 hours.** The images represent apoptotic nucleus with different concentrations of H_20_2 at 0 hours. The arrows (↖) represent the apoptotic nucleus found in each condition.

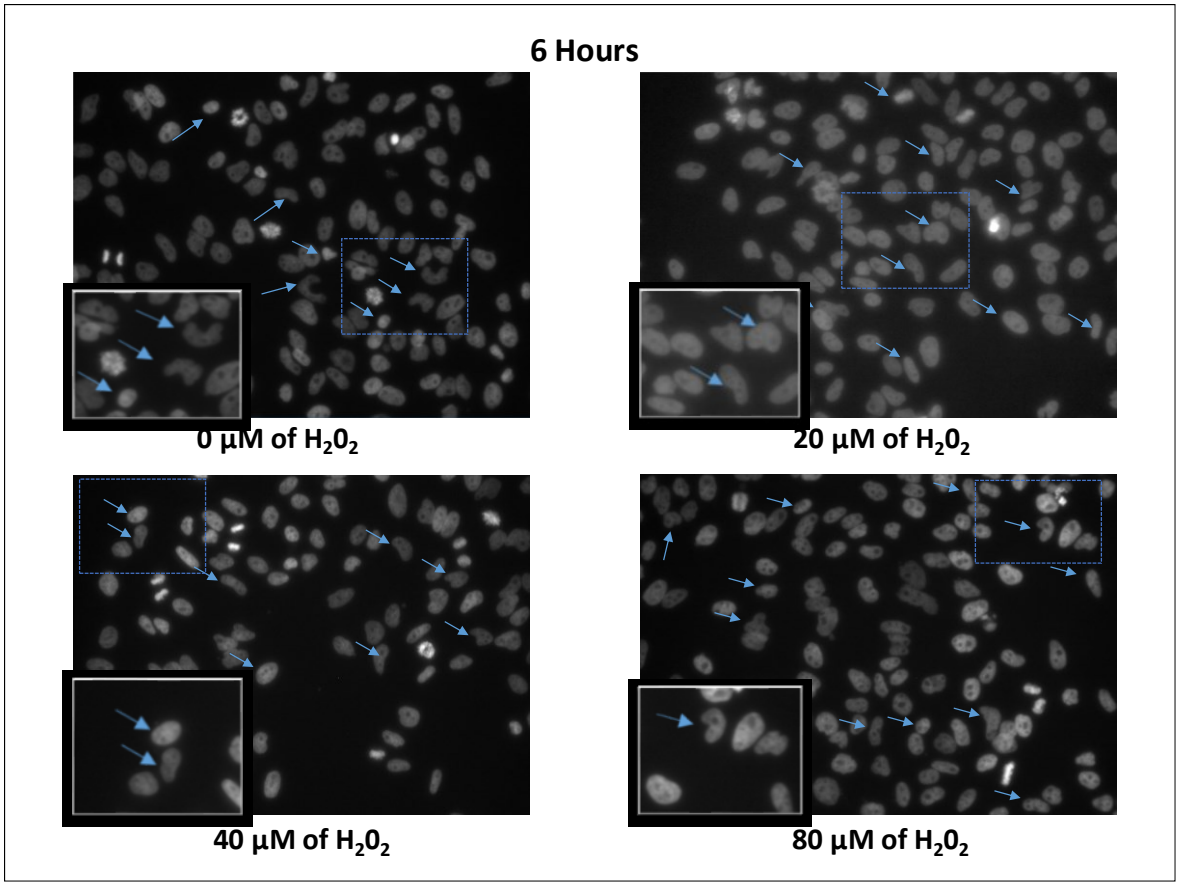

Figure 21. **Representative DAPI staining of apoptotic nucleus in different concentrations of H_2O_2 at 6 hours.** The images represent apoptotic nucleus with different concentrations of H_2O_2 at 6 hours. The arrows (↖) represent the apoptotic nucleus found in each condition.

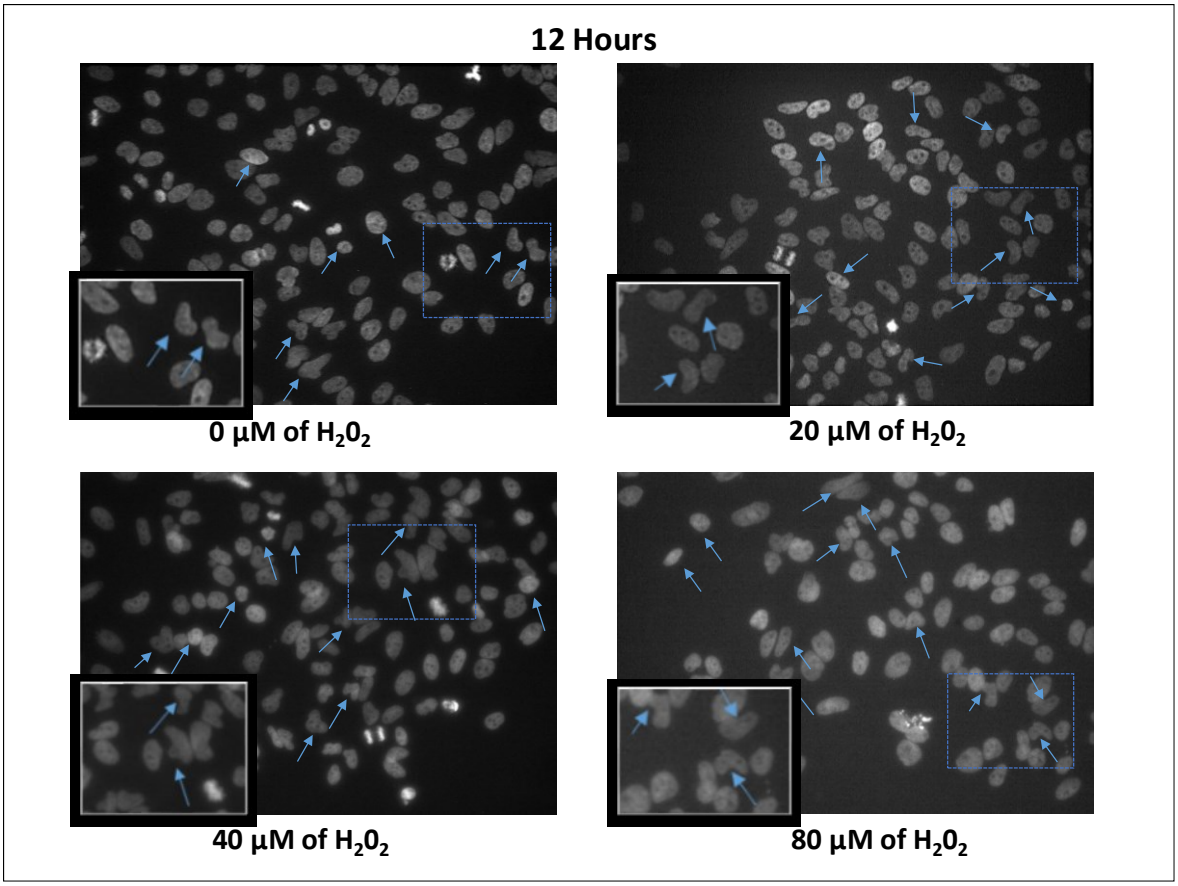

Figure 22. **Representative DAPI staining of apoptotic nucleus in different concentrations of H_2O_2 at 12 hours.** The images represent apoptotic nucleus with different concentrations of H_2O_2 at 12 hours. The arrows (↖) represent the apoptotic nucleus found in each condition.

To calculate the percentage of apoptotic nucleus, we considered the three types of apoptotic nucleus that are described in literature[91], namely chromatin condensation, nuclear fragmentation and nuclear condensation. The counting in each condition was always compared with controls. In all conditions, nucleus with chromatin condensation and nuclear fragmentation were not found. Overall, apoptotic nucleus presented a reduction in nuclear size and a structure similar to pyknosis (nuclear condensation) (Figure 20-22). The percentage of apoptotic cells was calculated for each condition (Figure 23).

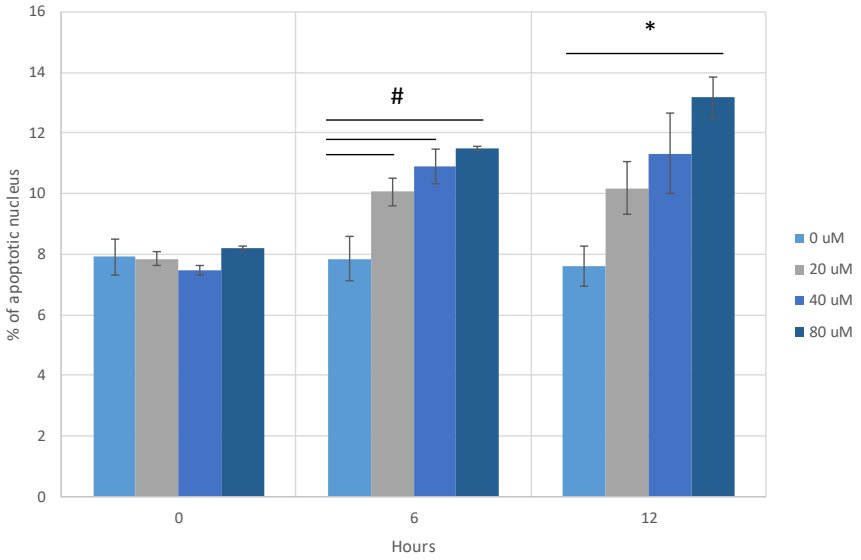

Figure 23. **Percentage of apoptotic nucleus.** Cells were treated with the indicated concentrations of H_2O_2 for 0h, 6h and 12 hours. Results present the percentage of apoptotic nucleus calculated in each condition. Data are presented as the mean ±SEM of at least three independent experiments (n=3). #/* $p < 0.05$ statistic symbols: # for comparisons between 0µM and 20µM, 0µM and 40µM and 0µM and 80µM of H_2O_2 at 6 hours, using one-way ANOVA followed by the Dunnets test, * for comparisons between 0µM and 80µM of H_2O_2 at 12 hours, using one-way ANOVA followed by the Dunnets test.

The percentage of apoptotic nucleus at the 0 hours' time point is essentially similar, around 8% (Figure 23). At the 6 hours' time point, there is a significantly increase to 10-11% of apoptotic cells in each condition (20, 40 and 80 µM) ($p < 0.05$, by one-way ANOVA followed by the Dunnets test) (Figure 23 and Appendix 1B). At the 12 hours' time point, it was also observed an increase of apoptotic cells in each condition, being with 80 µM of H_2O_2 registered the highest percentage of apoptotic cells, around 13% (Figure 23). After this analysis, we conclude that there a significantly increase of percentage of apoptotic nucleus with 80µM of H_2O_2 at 12 hours ($p < 0.05$, by one-way ANOVA followed by the Dunnets test) (Figure 23 and Appendix 1B). Next, we decided to evaluate the intracellular levels of both TRF2 and LAP1 and consequently the role of LAP1:TRF2 complex in the same conditions. Simultaneously, a marker of DNA damage was also monitored in the same conditions.

4.3.4 Detection of cellular DNA damage induced by H_2O_2

H2AX is phosphorylated by ATM on its Ser139 site. The phosphorylation of H2AX (γ-H2AX) at the Ser139 is considered a hallmark of DNA damage, namely for DSBs[64]. To further investigate the DNA damage induced by H_2O_2, HeLa cells were incubated with

different concentrations of H_2O_2, namely 0, 20, 40 and 80µM. The cells were harvested in different times points (0, 6, 12 hours) and further analyzed by SDS-PAGE and immunoblotting using anti-γ-H2AX Ser139 antibody. The results are presented in figure 24.

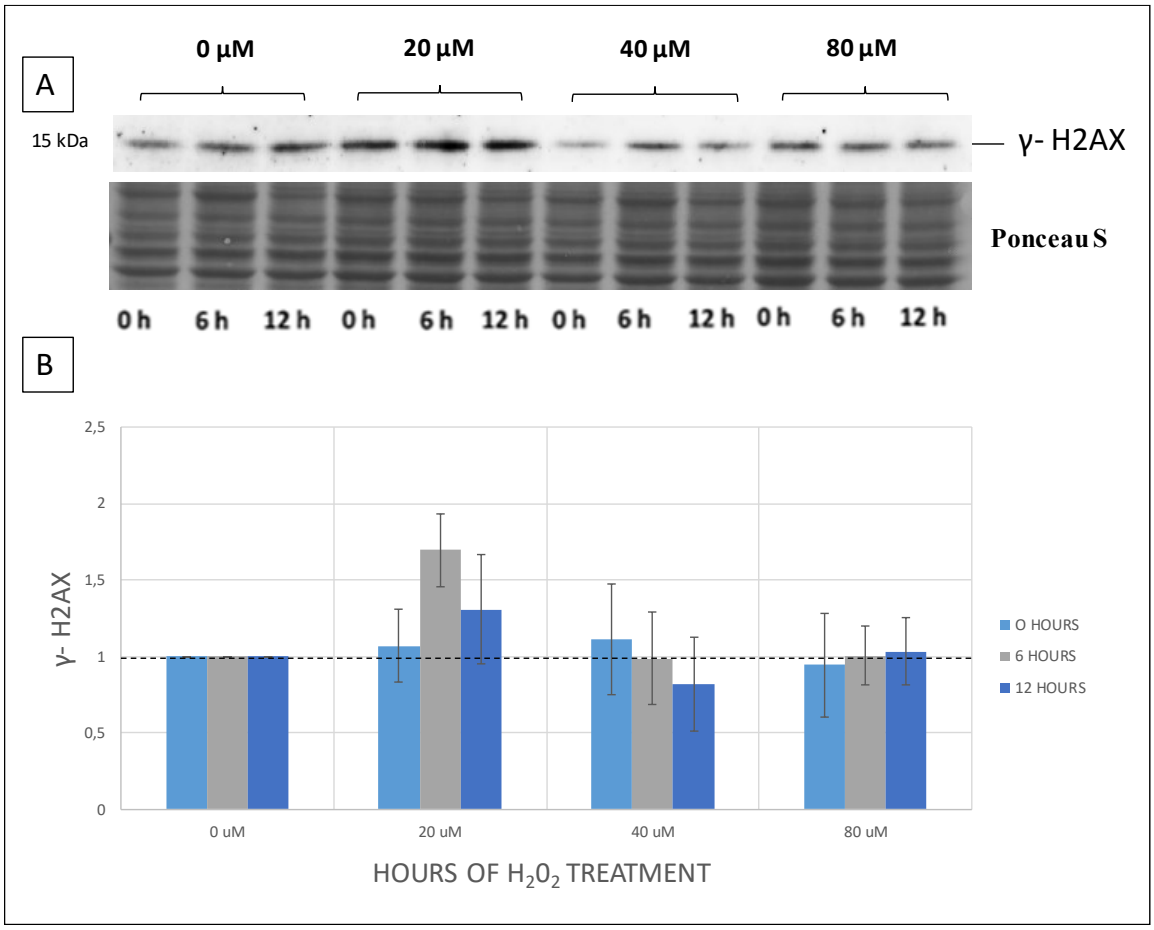

***Figure 24.* γ-H2AX expression in HeLa cells upon H_2O_2 exposure.** Cells were treated with the indicated concentrations of H_2O_2 for 0, 6 and 12 hours. Cell lysates were collected and analyzed by immunoblotting with anti-γ-H2AX Ser139 antibody. **A-** Immunoblot of cell lysates probed with anti-mouse monoclonal γ-H2AX Ser139. **B-** Quantification of γ-H2AX levels in HeLa cells upon H_2O_2 exposure. Data are presented as the mean ± SEM of at least three independent experiments (n=3).

The phosphorylation of H2AX (γ-H2AX) increase in the presence of 20 µM of H_2O_2 condition, mainly at 6 hours (Figure 24). Concentrations with 40 µM and 80 µM of H_2O_2 not seems changes in the levels of γ-H2AX (Figure 24).

4.3.5 Evaluate the expression levels of the LAP1:TRF2 complex during DNA damage

TRF2 is a protein associated with DNA damage response and telomere signaling[83,87] and it was identified in this study as a novel LAP1 interactor (as shown in the previous sections), therefore, the physiological function of this complex should be presumed. The expression levels of both LAP1 and TRF2 were evaluated during DNA damage response induced by H_2O_2 exposure. HeLa cells were incubated with different concentrations of H_2O_2, namely 0, 20, 40 and 80µM. The cells were harvested at different times points (0, 6, 12 hours) and further analyzed by SDS-PAGE and immunoblotting using anti-LAP1 and anti-TRF2 antibodies. The results are presented in figures 25 and 26.

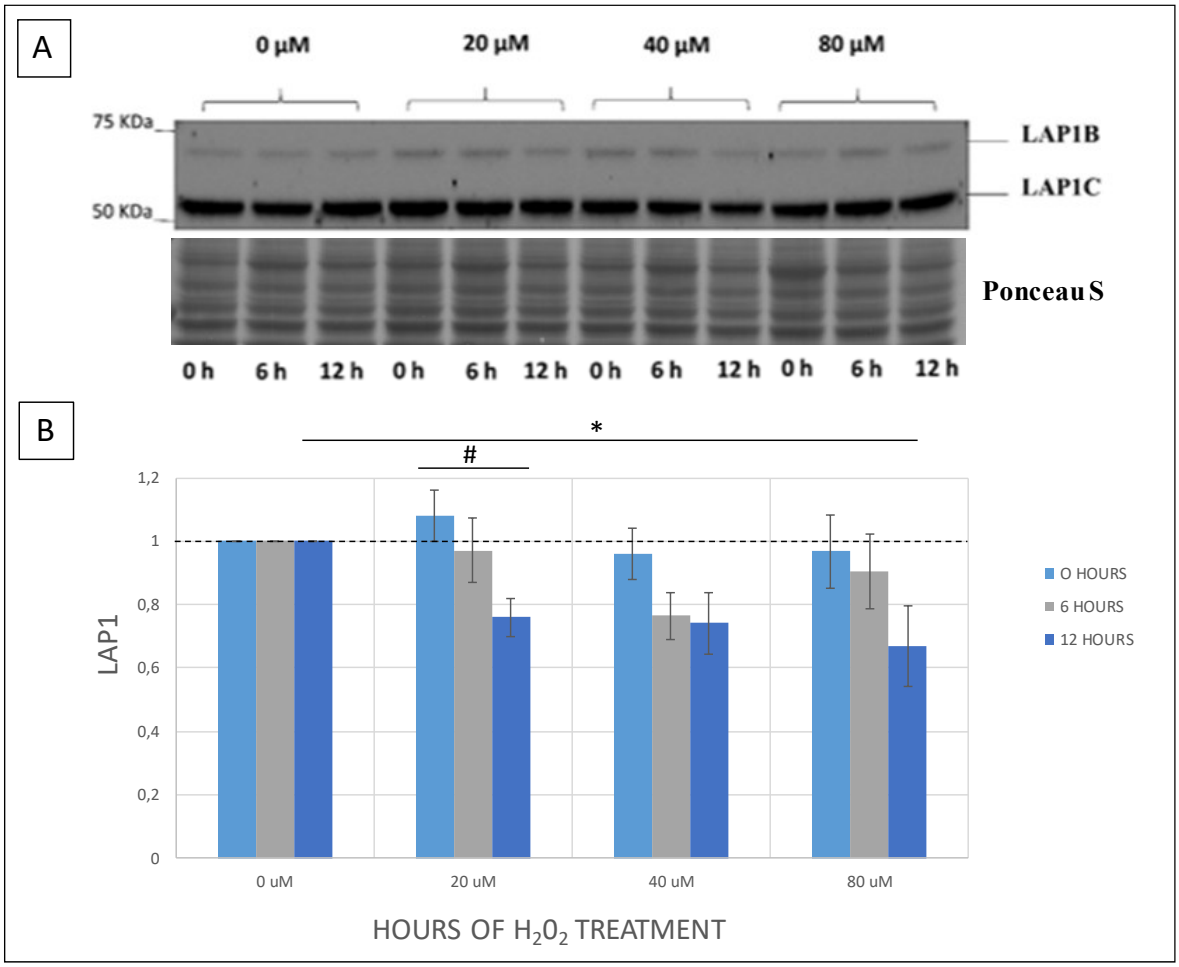

Figure 25. **LAP1 expression in HeLa cells upon H_2O_2 exposure.** Cells were treated with the indicated concentrations of H_2O_2 for 0, 6 and 12 hours. Cell lysates were collected and analyzed by immunoblotting with anti-LAP1 antibody. **A-** Immunoblot of cell lysates probed with anti-rabbit polyclonal LAP1. **B-** Quantification of LAP1 (LAP1B+LAP1C) levels in HeLa cells upon H_2O_2 exposure. Data are

presented as the mean ± SEM of at least five independent experiments (n=5). */# p< 0.05 statistic symbols: * for comparisons between 0µM and 80µM of H_2O_2 at 12 hours, using one-way ANOVA followed by the Dunnets test, # for comparisons between 0 and 12 hours' time points with 20 µM of H_2O_2, using one-way ANOVA followed by the Dunnets test.

When the cells were incubated with reduced concentrations of H_2O_2 (20µM), the expression levels of LAP1 significantly decrease at 12 hours' time point, comparatively to the control (0 hours) (p< 0.05, by one-way ANOVA followed by the Dunnets test) (Figure 25 and Appendix 1C). The effect observed in 40 µM is similar to 20 µM, but the reduction was not significantly (Figure 25). The 80 µM of H_2O_2 condition appears to induce a significantly decreasing of total LAP1 at 12 hours (p<0,05, by one-way ANOVA followed by the Dunnets test) (Figure 25 and Appendix 1C).

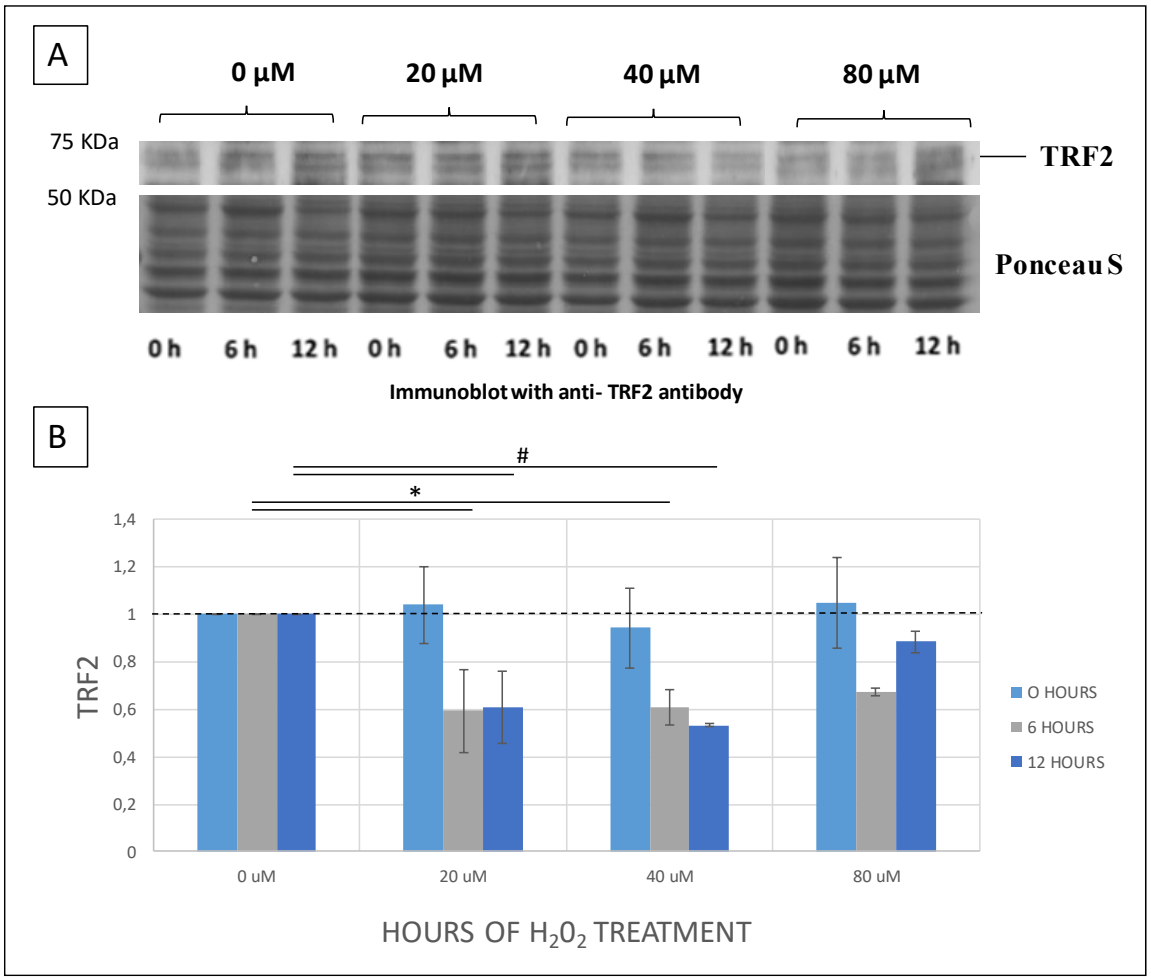

Figure 26. **TRF2 expression in HeLa cells upon H_2O_2 exposure.** Cells were treated with the indicated concentrations of H_2O_2 for 0, 6 and 12 hours. Cell lysates were collected and analyzed by immunoblotting with anti-TRF2 antibody. **A-** Immunoblot of cell lysates probed with anti-mouse monoclonal TRF2. **B-** Quantification of TRF2 levels in HeLa cells upon H_2O_2 exposure. Data are presented as the mean ±

SEM of at least three independent experiments (n=3). */# $p < 0.05$ statistic symbols: * for comparisons between 0μM and 20μM, 0μM and 40μM of H_2O_2 at 6 hours, by using one-way ANOVA followed by the Dunnets test, # for comparisons between 0μM and 20μM, 0μM and 40μM of H_2O_2 at 12 hours, by using one-way ANOVA followed by the Dunnets test.

Both 20 and 40 μM of H_2O_2 concentrations induce a significant reduction of TRF2 expression in all time points ($p<0.05$ one-way ANOVA followed Dunnets test) (Figure 26 and Appendix 1C). With the highest H_2O_2 concentration (80 μM) the expression levels of TRF2 decreases at 6 hours' time point and apparently increases at 12 hours' time point (Figure 26).

4.3.6 Evaluation of the subcellular distribution of LAP1 and TRF2 during DNA damage

To further address the physiological relevance of LAP1:TRF2 complex during DNA damage, the subcellular distribution and co-localization of both proteins in HeLa cells was analyzed. HeLa cells were plated in 12-well plates at cell density of 1.6×10^5 cells per well and cultured for 16 hours at 37ºC in a humidified 5% CO_2 chamber. After 16 hours, the cells were incubated with 80 μM of H_2O_2 for 12 hours, alongside with control condition. After that period, the cells were fixed and proceeded for ICC. To monitor the presence of DSBs induced by H_2O_2 indirect immunofluorescence visualization of γ-H2AX was used. This histone forms discrete foci in chromatin containing DSB[87]. LAP1 was stained with anti-LAP1 antibody (labelled with green Alexa 488), TRF2 was stained with anti-TRF2 antibody (labelled with red Alexa 594) and γ-H2AX was stained with anti-γ-H2AX Ser139 antibody (labelled with red Alexa 594) (Figure 27 and 28). The samples were mounted on a microscope slide with DAPI-containing VECTASHIELD® Mounting media. Fluorescence micrographs were taken by using a fluorescent microscope, Olympus IX-81 (Olympus, Optical Co. GmbH).

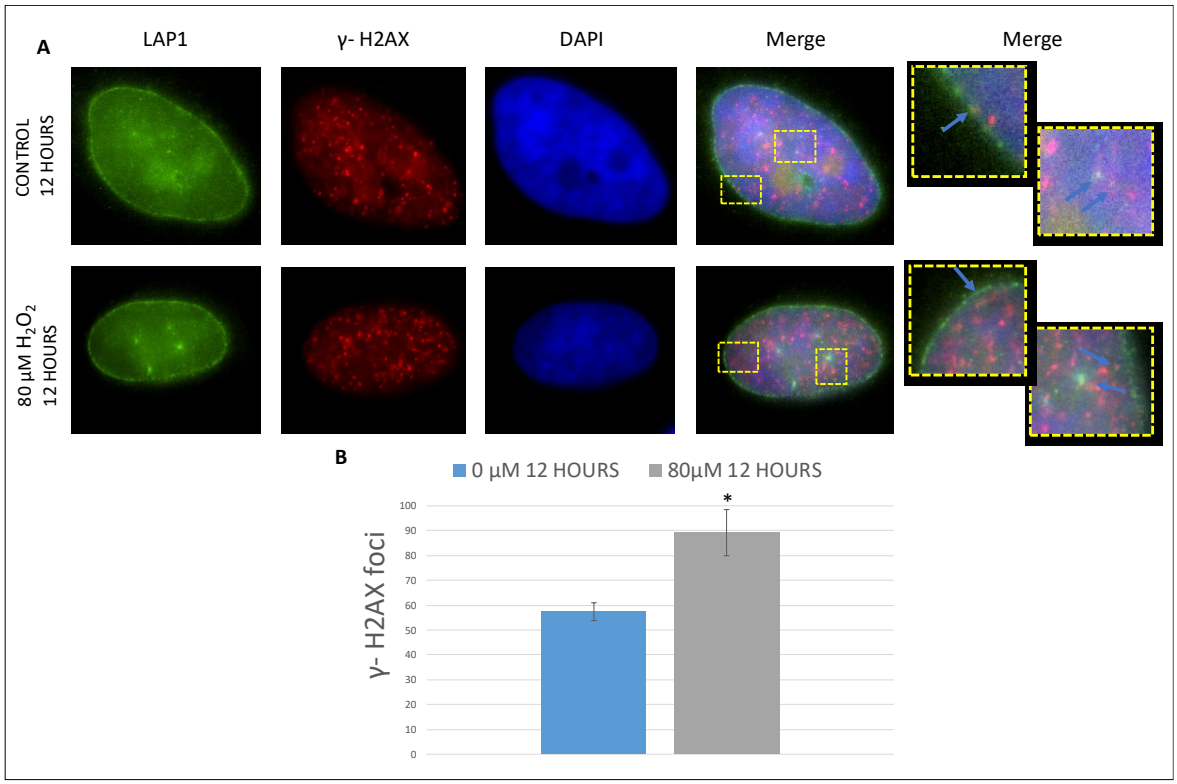

Figure 27. Subcellular distribution of LAP1 and γ-H2AX in HeLa cells. Cells were treated with 80 µM of H_20_2. The control condition also was prepared. At 12 hours, the cells were fixed. LAP1 was stained with anti-LAP1 antibody (labelled with green Alexa 488) and γ-H2AX was stained with anti-γ-H2AX Ser139 antibody (labelled with red Alexa 594). The nucleus was stained with DAPI. A) Co-localization of LAP1 with γ-H2AX with 0 and 80 µM of H_20_2. The co-localization of LAP1, γ-H2AX and DAPI staining can be observed in the merged figures (arrows). B) Quantification of γ-H2AX foci at control and 80 µM of H_20_2. Data are presented as the mean ±SEM of at least three independent experiments (n=3). * $p< 0.05$ statistic symbols: *for comparisons between 0µM and 80µM of H_20_2 at 12 hours, using t-test.

As previously described, LAP1 is a NE protein responsible by NE maintenance[40]. This protein is located mainly in the NE and in some points in the nucleus itself, as shown in Figure 27A. γ-H2AX was found mainly in the nucleus. This histone forms discrete foci in chromatin and each foci represents DSBs[87] (Figure 27A). Co-localization of LAP1 with γ-H2AX in two conditions (0 and 80µM of H_20_2 at 12 hours) was observed at several subnuclear structures and at specific points near of the NE (Figure 27A).

To detect DNA damage and repair *in situ* in individual cells for each condition, we decided count the number of the γ-H2AX foci per cell (Figure 27B). These quantitative results allowed the detection of γ-H2AX in chromatin (red spots in Figure 27B), these spots indicated DSBs[99]. In the control, ±60 γ-H2AX foci per cell were counted while in the 80 µM condition ±90 γ-H2AX foci were found (Figure 27B). The concentration of 80 µM of H_20_2

at 12 hours leads to a significantly increase of γ-H2AX foci per cell, when compared with the control ($p < 0.05$, by t-test) (Figure 27B and Appendix 1D).

After this analysis, we decided to co-localize LAP1 with TRF2 in the same conditions. TRF2 is a novel LAP1 interacting protein (as showed above) and in response to DNA damage it migrates to specific sites of DNA damage, namely DSBs and co-localizes with DSBs[87].

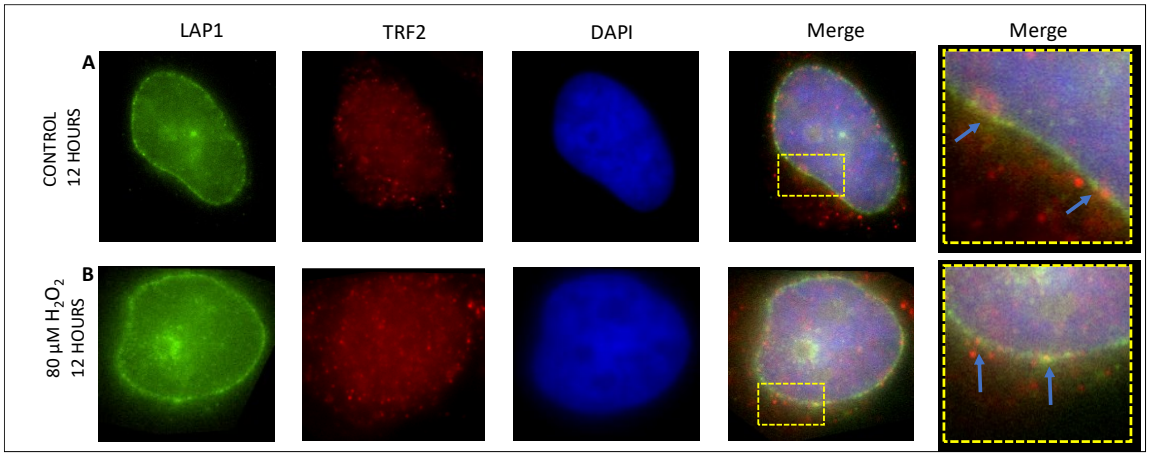

Figure 28. **Subcellular distribution of LAP1 and TRF2 in HeLa cells**. Cells were treated with 80 µM of H_20_2. The control condition also was prepared. At 12 hours, the cells were fixed. LAP1 was stained with anti-LAP1 antibody (labelled with green Alexa 488) and TRF2 was stained with anti-TRF2 antibody (labelled with red Alexa 594). The nucleus was stained with DAPI. A) Control co-localization of LAP1 with TRF2. B) Co-localization of LAP1 with TRF2 with 80 µM of H_20_2. The co-localization of LAP1, TRF2 and DAPI staining can be observed in the merged figures (arrows).

LAP1 is located mainly in the NE, as previously described (Figure 28). TRF2 is enriched mainly in the nucleus of HeLa cells in two conditions but some immunoreactivity in the cytoplasm was also observed (Figure 28). The co-localization between LAP1 and TRF2 was observed mostly at several points near of the NE in the two conditions (Figure 28).

4.4 Potential role of LAP1:TRF2 in cell cycle progression

LAP1 seem to play a fundamental role during mitosis, since it maintains the NE structure and it is involved in cell cycle progression. In interphasic cells, LAP1 was found associated to lamins and chromosomes[40]. TRF2 is a protein located in chromosome ends and it is essential for the protection of all chromosomes in all steps of cell cycle[100]. Both proteins appear to be associated with cell cycle progression. Therefore, we decided to evaluate the LAP1:TRF2 complex during cell cycle progression in HeLa cells. To address this purpose, we plated HeLa cells at cell density of 1.6×10^5 cells per well. The plate was incubated at 37ºC with 5% CO_2 for 16 hours. Upon this period, the cells were fixed. LAP1 was stained with anti-LAP1 antibody (labelled with green Alexa 488) and TRF2 was stained with anti-TRF2 antibody (labelled with red Alexa 594) (Figure 29). The samples were mounted on a microscope slide with DAPI-containing VECTASHIELD® Mounting media. Fluorescence micrographs were taken by using a fluorescent microscope, Olympus IX-81 (Olympus, Optical Co. GmbH).

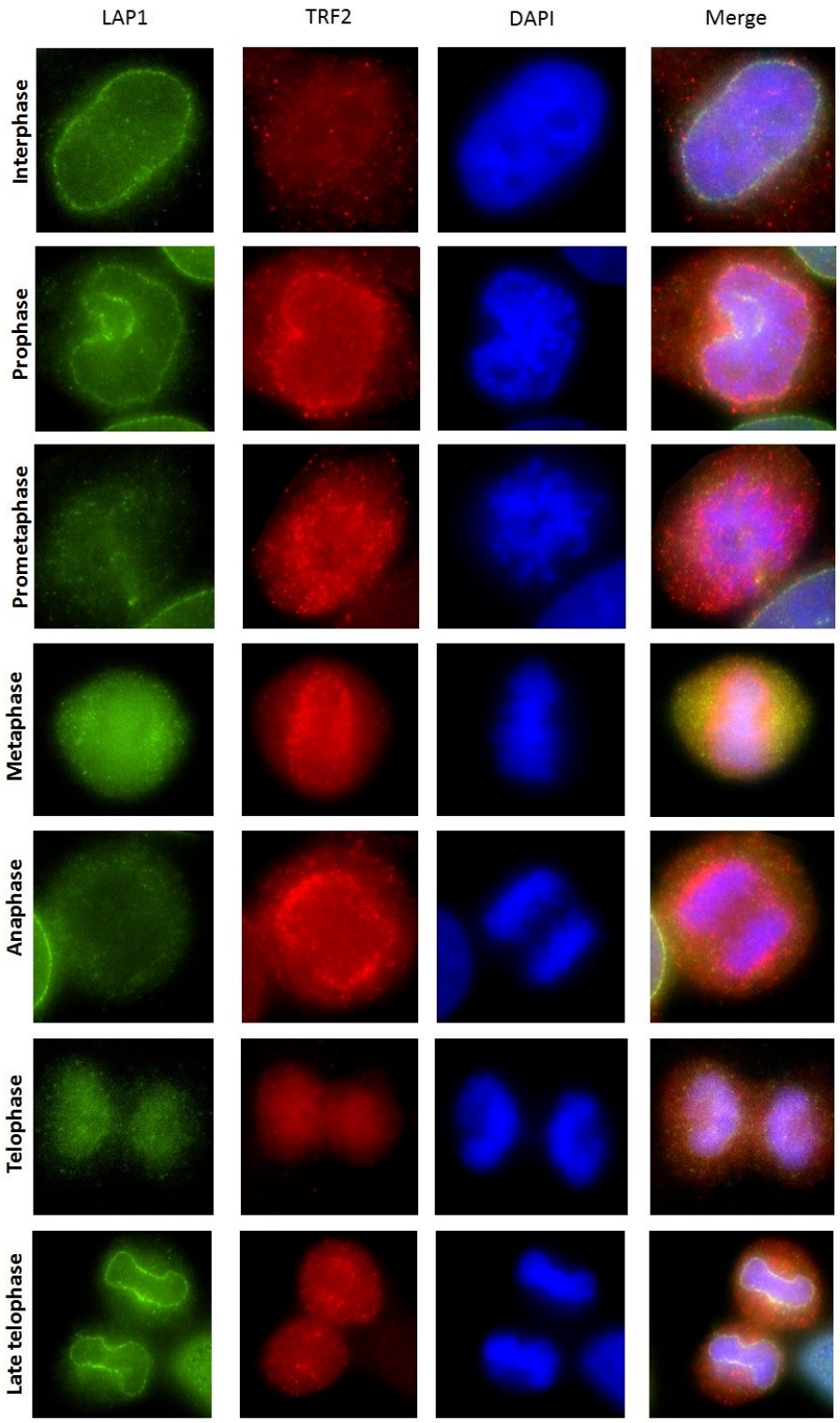

Figure 29. **Subcellular distribution of LAP1 and TRF2 in HeLa cells during cell cycle progression.** LAP1 was stained with anti-LAP1 antibody (labelled with green Alexa 488) and TRF2 was stained with anti-TRF2 antibody (labelled with red Alexa 594). The nucleus was stained with DAPI. The co-localization of LAP1, TRF2 and DAPI staining during cell cycle progression can be observed in the merged figures.

During interphase, LAP1 is localized at the nuclear periphery in accordance with its location in the INM and TRF2 is found mainly in the nucleus (Figure 29). The co-localization of these two proteins in this phase occurs in some points near of NE (Figure 29). In the initial phase of mitosis (prophase), LAP1 begins to disperse with the NE and TRF2 is dispersed from the nucleus to the nuclear periphery (Figure 29). In this phase, the co-localization between these two proteins occurs mainly in NE (Figure 29). In prometaphase, an intermediary phase between prophase and metaphase, LAP1 does not appear to have NE localization and TRF2 localizes mainly around the nucleus (Figure 29). At metaphase, LAP1 appears to be distributed through the cell in a punctuated pattern, excluding the chromosomal area while TRF2 is also found around the chromosomal area (Figure 29). In anaphase, LAP1 appears to have the same localization as in metaphase while that TRF2 appears to be found around of chromosomal area where it co-localizes with LAP1 in cytoplasm (Figure 29). At initial stages of telophase, LAP1 is found around condensated chromosomes and TRF2 is present in the condensated chromosomal areas. Both proteins co-localize in the nuclear periphery (Figure 29). In late telophase, LAP1 is found in the NE and TRF2 locates mainly in the nuclear area but also in same points of the NE (Figure 29). At the end of mitosis, the two proteins co-localize in the nuclear periphery (Figure 29).

Discussion

5. Discussion

LAP1 is an ubiquitously expressed protein encoded by the *TOR1AIP1* gene and located at the INM[26]. LAP1 was identified using a monoclonal antibody generated against lamina-enriched fractions of rat liver nuclei. This antibody recognizes three members of LAP1, namely LAP1A, LAP1B and LAP1C that are a result of alternative splicing of the *TOR1AIP1* gene[26,36,37]. However, in humans only 2 isoforms are known, LAP1B and LAP1C[38]. The exact physiological function of LAP1 is unknown, LAP1 has been associated to several functions through its binding to several proteins. Several LAP1 functions were described, such as, nuclear architecture maintenance and chromatin regulation in association to lamins, regulation of cell cycle progression by binding to PP1, regulation of torsinA ATPase activity, NE localization of torsinA and NE dynamics by binding to torsinA and also in NE integrity and skeletal muscle maintenance by the interaction with emerin[39]. Recently, a study from our group allowed for the identification of several novel putative LAP1 functionally associated proteins, namely TRF2, RAP1, RIF1, ATM, MAD2L1 and MAD2L1BP. Some of these proteins are involved in DNA damage response and telomere signaling[45].

5.1 Identification of TRF2 as a novel LAP1 interactor

Telomeres are protective caps responsible for the protection of chromosomal ends in order to maintain genomic integrity[69]. The structure of telomeres and its signaling functions are regulated by a complex termed the shelterin complex[101]. This complex comprises six proteins, among these are TRF2 and RAP1. These two proteins appear to be novel putative LAP1 interactors[45]. In order to assess this interaction co-immunoprecipitation assays were performed. This technique is used to validate protein interactions by formation of antigen-antibody complexes[96]. Several co-immunoprecipitations using specific antibodies directed against LAP1, TRF2 and RAP1 were performed. LAP1 binds to TRF2, confirming that TRF2 as a novel LAP1 interactor (Figure 14). Furthermore, we also established that RAP1 does not co-immunoprecipitates with LAP1. As expected, Rap1 was able to co-immunoprecipitates with TRF2 and the same result was obtained when RAP1 antibody was used to co-immunoprecipitation. This is in agreement with previous results where the interaction was established[81] (Figure 15 and 16). LAP1C was co-immunoprecipitated with

TRF2 and RAP1 (Figure 15 and 16). However, this isoform was also detected in the negative controls (Figure 15 and 16). LAP1C appears to bind non-specifically to Dynabeads and Dynabeads plus Mouse IgG, therefore these results are inconclusive. Future experiments will be necessary to increase the number of samples, prolong the washing steps, change the Dynabeads used, or decrease incubation time (Dynabeads and sample) during the Co-Immunoprecipitation assay. Overall co-immunoprecipitations, LAP1B was not detected, since this isoform is less abundant in both human cell lines and in tissues, as previously reported[38]. In the future, to detect this isoform (LAP1B) will be necessary to increase the amount of protein used for each co-immunoprecipitation experiment. Given that the results with LAP1 antibody were very clear we are very confident that TRF2 and not RAP1 is a novel LAP1 binding protein. To further pursued this idea co-immunoprecipitations of LAP1 were performed in cells incubated with different concentrations of OA (0, 0.25 and 500 nM). The samples were separated by SDS-PAGE and the bands correspondent to LAP1C (56 kDa) and LAP1B (68 kDa) were excised and analyzed in a Nano-HPLC coupled to a Q Exactive mass spectrometer. Essentially, we analyzed the presence of peptides correspondent to TRF2 and RAP1 peptides in each condition. Only two TRF2 peptides were identified in co-immunoprecipitation of LAP1, on cells incubated with 500 nM of OA (Table 5). The OA is an inhibitor of the serine and/ or threonine phosphatases. The 500 nM of OA inhibits both PP1 and PP2A[102]. Protein-protein interactions are regulated by mechanisms of protein phosphorylation, which involve protein kinases and phosphatases. PP2A and PP1 are serine/threonine phosphatase responsible for the dephosphorylation of more than one-third of proteins in eukaryotic cells. Recently, a study from our group established that LAP1 is a novel PP1 substrate and that PP1 dephosphorylates LAP1 on Ser306 and Ser310[37,38]. When PP1 and PP2A are inhibited, LAP1 becomes phosphorylated and apparently binds more to TRF2. However, to confirm this results phosphorylation assays should be performed.

In conclusion, TRF2 is a novel LAP1 interactor, however further experiments will be necessary to confirm this result.

5.2 Potential role of LAP1:TRF2 during DNA damage

To understand the physiological role of LAP1 it is crucial to validate novel LAP1 binding proteins and determine their dual cellular functions. TRF2 is a shelterin component required to prevent mammalian telomeres from activating DNA damage checkpoints[83]. This protein has been reported to anchor the shelterin complex to double-stranded telomeric DNA[103] and is crucial in the end-protection of chromosomes by suppression of ATM activation, namely by inhibition of autophosphorylation of ATM kinase on Ser1981[79,83]. TRF2 interacts with RAP1 (as showed in the results of this thesis, Figure 15) forming a complex[77]. This complex is associated with a set of key proteins involved in DNA damage responses, namely ATM, MRN complex, Ku, DNA-PKcs, WRN, BLM[77,86]. In fact, the involvement of telomeres in cellular responses to DNA damage has been explored[83]. TRF2 has been described as a protein that associates the telomeres to proteins that are involved in DSBs repair[84,87]. The non-telomeric role of TRF2 in response to DNA damage remains to be determined, but it is actually known that this protein is phosphorylated by ATM and interacts with DSBs, migrating to these sites in response to DNA damage[84,87]. LAP1 appears to also be associated to ATM kinase. During mitosis, LAP1 is regulated by mechanisms of phosphorylation that involve the action of several kinases that regulate the cell cycle, among them is ATM[40]. Both LAP1 and TRF2 seem to have in common the binding to ATM kinase as a regulatory mechanism. To further investigate the potential relevance of the LAP1:TRF2 complex, we decided to evaluate the putative role of this complex in response to stimulation of ATM kinase activity upon DNA damage. ATM activation is caused by DSBs. The DSBs are originated by multiple factors, including oxidative stress[58,60]. When the cells are exposed to these agents, DSBs are originate and recognized by a complex, termed the MRN complex. The MRN complex regulates the activation of ATM which phosphorylates and recruits downstream effectors, namely BRAC1, 53BP1, H2AX, p53, CHK2, FANCD2, SMC1 and BLM1[62]. Oxidative stress causes different types of DNA damage, among these are DSBs. The activation of ATM by H_20_2 has been well documented, however, the capacity of H_20_2 to induce DNA damage through others mechanisms has been controversial[104,105]. H_20_2 is a ROS involved in ATM activation, H2AX phosphorylation and DSBs generation[91]. To study the concentrations and time points of H_20_2 treatment that would induce DNA damage, optimization of HeLa cells growth upon H_20_2 exposition was performed (Figure 17 and 18). The 0, 20, 40 and 80 μM of H_20_2 concentrations were chosen and 0, 6 and 12 hours were the

times points selected to investigate the role of the LAP1:TRF2 complex during DNA damage (Figure 19). At 12 hours, all the concentrations of H_20_2 present variability on number of viable cells (Figure 19). Additionally, in this time point with 80 μM of H_20_2 a significant reduction of cell viability cell was observed ($p< 0.05$, by one-way ANOVA followed by the Dunnets test) (Figure 19 and Appendix 1A). Therefore, to assess the effect of H_20_2 in the apoptotic mechanism, the percentage of apoptotic nucleus in each condition was measured (Figure 20-22). The highest percentage of apoptotic nucleus was measure in 80μM of H_20_2 at 12 hours (around 13%) ($p< 0.05$, by one-way ANOVA followed by the Dunnets test) (Figure 23 and Appendix 1B). To confirm these results, it will be necessary to perform a new assay to detect DNA fragmentation, for example, by using the TUNEL assay.

DNA damage induced by H_20_2 was monitored through western blot analysis of γ-H2AX (Figure 24). γ-H2AX is considered a hallmark of DNA damage, namely DSBs[64]. In response to the formation of DSBs, this histone is phosphorylated in Ser139 by ATM[64,99]. In this study, the γ-H2AX Ser139 increases with concentration of 20μM of H_20_2, at 6 hours. However, the results of γ-H2AX are not statistically significant. To confirm DNA damage induced by H_20_2 it will be necessary to monitor DNA damage through others assays, such as the Comet assay. After detection of DNA damage induced by H_20_2, the expression of LAP1 and TRF2 was evaluated in same conditions. The expression of LAP1 was significantly decrease in 20μM and 80μM at 12 hours comparatively to the control ($p< 0.05$, by one-way ANOVA followed by the Dunnets test) (Figure 25 and Appendix 1C). Interestingly, the expression of TRF2 is also significantly reduced at 6 and 12 hours with 20 and 40μM of H_20_2, relative to control ($p< 0.05$, by one-way ANOVA followed by the Dunnets test) (Figure 26 and Appendix 1C). Previous studies have shown that TRF2 association with DSB is temporary, TRF2 associates with DSB induced by a DNA intercalator (laser microbeam irradiation) within 2 seconds of irradiation. TRF2 decreases exponentially at sequential time points[87]. These findings suggest that TRF2 is expressed at initial stages of DSB formation and LAP1 seems to have an expression profile similar to TRF2.

In conclusion, lower concentrations of H_20_2 leads to DSBs, increasing the phosphorylation status of H2AX on Ser139. In response to DSBs formation, the expression of LAP1 and TRF2 decreases significantly.

5.3 Subcellular distribution of LAP1 and the novel interacting protein TRF2 during DNA damage

We established that LAP1:TRF2 complex is formed *in vitro* and we assume that both proteins might participate in cellular functions. Therefore, it is important to determine the subcellular distribution of these proteins and also the specific structures that they are associated. To evaluate the localization of LAP1 and γ-H2AX complex during DNA damage, co-localization of LAP1 with γ-H2AX in HeLa cells (0 and 80μM H_20_2 during 12 hours) was performed (Figure 27A). LAP1 locates mainly in the NE and in some points in the nucleus itself, as previously reported[40] (Figure 27A). The immunostaining of γ-H2AX in cells is marked with discrete foci in chromatin containing DSBs, as previously reported[87] (Figure 27A). In control (12 hours) ±60 foci per cell were counted, while in the 80μM condition (12 hours) the registered number of foci per cell was significantly superior around ±90 ($p< 0.05$, t-test) (Figure 27B and Appendix 1D). In response to 80μM of H_20_2, LAP1 co-localizes with γ-H2AX in the DSBs and in specific points near to the NE (Figure 27A). The same was observed in the control condition (Figure 27A). However, to confirm these results it will be necessary to increase the number of experiments (n) for each condition. After co-localization of LAP1 and γ-H2AX, the co-localization of the LAP1 with TRF2 was performed under the same conditions. TRF2 exhibited an enriched localization to the nucleus (Figure 28). In response to DNA damage, TRF2 co-localizes with DSBs as previously reported[87]. Co-localization between these two proteins was observed mostly at specific points near of the NE (Figure 28). However, to verify these results it will be necessary to increase the number of experiments (n) for each condition. In these studies, the concentrations and the time points were chosen before optimization of γ-H2AX antibody for western-blot, as a future perspective it will be necessary to repeat this assay analyzing new concentrations and time points that in fact correspond to DNA damage, namely 20μM of H_20_2 at 6 hours, since in this concentration H2AX phosphorylation reaches a peak.

In conclusion, LAP1 co-localizes with γ-H2AX in some points of the NE and nucleus, in response to DNA damage. Additionally, LAP1 co-localizes with TRF2 in the nuclear periphery. However, to strengthen these conclusions it will be necessary to repeat this experiment in future, with a new concentration of H_20_2, namely 20μM of H_20_2 at 6 hours.

5.4 Role of LAP1:TRF2 complex in cell cycle progression

In eukaryotes, the chromosomes are enclosed by a double membrane which separates the nucleus from the cytoplasm, the NE. This physical barrier separates the chromosomes from cytoplasmic structures[106]. During cell division, the NE suffers an extensive transformation in its architecture to ensure that segregated DNA is enclosed in a single cell nucleus in each daughter cell[107]. In the beginning of mitosis, the NE is completely disassembled and it reassembles again at the end of mitosis. The NE breakdown is a dynamic mechanism that allows chromosomes to access the microtubule spindle and involves a set of processes that include disassembly of NPCs, depolymerization of lamins and spreading of the NE soluble components and INM proteins to the cytoplasm and ER. The reassembly of the NE in the end of mitosis is marked by the concentration of the INM proteins and lamins on the decondensing chromatin, lamin polymerization and NPC assembly[40,107]. LAP1 is an integral protein of the INM crucial to the maintenance of the NE structure and cell cycle progression[40]. TRF2 is a ubiquitous protein present in more than 100 copies per chromosome end and it is crucial for protection of all chromosomes in all steps of cell cycle[78,100]. Both proteins appear to be associated with cell cycle progression. In order to evaluate the localization of the LAP1:TRF2 complex during cell cycle progression, co-localization between LAP1 and TRF2, in HeLa cells, was performed. During interphase, LAP1 is located in the nuclear periphery and in some points inside the nucleus where it associates to lamins and chromossomes[40] while TRF2 co-localizes with telomeres in interphasic nuclei[100]. In interphasic HeLa cells, LAP1 was also found in the NE and internal nuclear structures, while TRF2 was localized mainly to the nucleus (Figure 29). The co-localization between these two proteins during interphase was found in some points of the NE (Figure 29). At the end of interphase, the activation of mitotic kinases triggers the entry into prophase. This phase is characterized by a series of events: i) chromatin condensation, ii) formation of microtubules around the centrosomes, iii) chromosome separation, iv) retraction of INM proteins into ER, v) NPCs and lamins disassembly and vi) NE breakdown[107]. The breakdown of the NE allows the chromosomes to access the microtubule spindle for correct chromosome segregation[40]. During the prophase, TRF2 disperses away from the nucleus[108] and LAP1 localizes to the ER membranes, concomitant with nuclear lamins depolymerization[109]. In this study, LAP1 it is completely dispersed from the NE in prometaphase, as described in

literature[40] (Figure 29). TRF2 disperses away from the nucleus accumulating in nuclear periphery during prophase and prometaphase, as described in literature (Figure 29). During prophase and prometaphase, the co-localization between these proteins occurred essentially in the nuclear periphery (Figure 29). In metaphase, most of soluble NE components are located in the cytoplasm and the INM proteins concentrate in the tubular mitotic ER[107]. During this phase, LAP1 presents a punctuated pattern in the nucleus excluding chromosomal area[40] and TRF2 is found dispersed away, from condensed chromosomes[108]. The findings are in agreement with the literature, since LAP1 appears to be excluded from chromosomal area and TRF2 is dispersed from condensed chromosomes, locating mainly around them (Figure 29). The co-localization between both proteins occurs essentially throughout the cytoplasm (Figure 29). In the last steps of mitosis, the NE starts to reform its structure around chromatin. In anaphase, the chromatin begins to decondensate, the INM proteins remain dispersed into tubular mitotic ER and the NPCs reassemble[107]. In this phase, LAP1 occupies the same localization as in metaphase (Figure 29)[40]. The localization of TRF2 is unknown in this phase but it appears to be present around decondensating chromosomes while it co-localizes with LAP1 around nucleus (Figure 29). Throughout telophase, the NE reformation occurs and the INM proteins bind to DNA again while NPCs and lamins reassembly is achieved[107]. In the last steps of mitosis, LAP1 is found encircling the chromosomes even where they still not fully decondensed, this association to telomeres contributes to the NE reassembly through lamins which target chromosomes and anchor chromatin to the NE[40,110]. At an early stage of telophase, TRF2 re-entries into areas of decondensing chromosomes and returns to its initial position in the nucleus (nucleolus) at late telophase[108]. In this study, LAP1 surrounds the decondensating chromosomes in telophase while completely encircling the chromosomes in late telophase (Figure 29). In both phases, TRF2 localizes mainly in the nucleus (Figure 29). The co-localization between these two proteins occurs is some points of the NE, mainly at late telophase (Figure 29).

During mitosis, LAP1 co-localizes with acetylated α-tubulin in the mitotic spindle and γ-tubulin (organization of microtubules) in mitotic cells[40]. The role and association of TRF2 with these structures remains unknown. LAP1 is crucial for cycle progression, specifically in centrosome positioning. The knockdown of LAP1 causes a reduction of number of the mitotic cells, abnormal morphology of interphasic cells, alteration of acetylated α-tubulin distribution, formation of aberrant mitotic spindle and mitotic exit,

increasing of distance between the centrosomes and NE and reduction of γ-tubulin levels which results in microtubule instability[40].

In conclusion, LAP1 and TRF2 appear to be two proteins functionally associated to cell cycle progression. At the initial phases of the mitosis, when the NE breakdown occurs, TRF2 is recruited to the nuclear periphery and disperses around the condensed chromosomes. This dispersion could be related to the fact that chromosomes need to access the microtubule mitotic spindle. At end of mitosis, when the NE is reassembled TRF2 gets back to its initial position where it associates with decondensed chromatin. In all phases of mitosis, LAP1 and TRF2 appear to present a similar subcellular distribution, co-localizing in some points of NE in the initial and final steps of mitosis and in the nuclear periphery in the intermediate steps of mitosis. LAP1 and TRF2 are found in the nuclear periphery when the NE is disassembled and located to specific points of the NE when it is reassembled again. These results confirm that TRF2 can be a good candidate for the attachment of telomeres to the NE in somatic cells[111]. As future perspectives, it will be necessary to perform new immunofluorescence assays with the detection of other proteins involved in of cell cycle progression, namely, acetylated α-tubulin and γ-tubulin. Additionally, it would be interesting to analyze if the localization of TRF2 changes during cell cycle progression after the knockdown of LAP1. However, to confirm the role of this protein complex during mitosis it will be necessary increase the number of experiments (n) already performed. Finally, it would also be interesting to accomplish the LAP1 knockdown experiment in order to evaluate the TRF2 expression profile.

Concluding remarks

6. Concluding remarks

LAP1 is an integral membrane protein located in the INM. To date, its functions remain poorly understood, but several crucial cellular functions have been associated to LAP1 due to its interactions with some proteins, including lamins, torsinA, emerin and PP1. Several novel putative LAP1 interactors are emerging. In this study, TRF2 was identified as a novel LAP1 interactor. The work included in this thesis provides new physical and functional important associations of LAP1 to its newly described interactor TRF2, in response to DNA damage and in cell cycle progression.

In short, the co-immunoprecipitation and HPLC-MS assays allowed the identification of a novel LAP1 interactor, TRF2. TRF2 is a protein involved in telomere signaling, DNA damage response and cell cycle progression. In response to DNA damage, the expression of this complex is significantly reduced. During this, LAP1 possibly co-localizes with γ-H2AX in the DSBs and in some points of the NE and co-localizes with TRF2 in the nuclear periphery. This complex is also associated with cell cycle progression. When the NE is reassembled, the complex is located mainly in specific regions of the NE, evidencing that TRF2 allows the attachment of chromosomes to the NE membrane in somatic cells. Several experiments are still needed to performed and further explored these results, but we believe that this work will help advance the knowledge of the biological and molecular functions of the LAP1:TRF2 complex, particularly, in DNA damage response and cell cycle progression.

In conclusion, this work results in:

- Validation of TRF2 as a novel LAP1 interactor;
- Unravelling the potential role of LAP1 and TRF2 in response to DNA damage;
- Determining the subcellular distribution of LAP1 and its novel interacting protein TRF2, during DNA damage;
- Unravelling the potential role of LAP1:TRF2 complex during progression of cell cycle.

Future perspectives:

- To confirm the effect of H_20_2 in the induction of apoptosis by the TUNEL assay;
- To verify the detection of DNA damage induced by H_20_2 by the Comet assay;
- As LAP1 is phosphorylated by ATM during mitosis, it will be necessary evaluate the phosphorylation status of LAP1 in response to DNA damage using Phostag SDS PAGE method or manufacturing an antibody for phosphorylated LAP1;
- To further investigate if LAP1 and TRF2 interact in response to DNA damage, it will be interesting to perform co-immunoprecipitations of LAP1 and TRF2 incubated with H_20_2 (20 μM during 6 hours) and immunoblotted with anti-TRF2 and anti-LAP1 respectively;
- To detect subcellular distribution of this complex in response to DNA damage, it will be necessary to perform new immunofluorescence assays with new concentrations of H_20_2, namely 20 μM of H_20_2 during 6 hours;
- To confirm the association of this complex in response to DNA damage, it will be interesting to induce DNA damage by other methods, namely using Etoposide;
- To accomplish a complete study of the complex formed between LAP1 and TRF2 during progression of cell cycle it will be necessary to perform new immunofluorescence assays with detection of other proteins involved in progression of cell cycle, for example, acetylated α- tubulin and γ-tubulin;
- To confirm the results obtained from immunofluorescence assays it will be necessary to increase the number of experiences (n) and take photos with confocal microscopy to thoroughly quantify the percentage of co-localizations between both proteins;
- It will be interesting to perform LAP1 knockdown, in order to investigate the localization status of TRF2 during cell cycle progression with immunofluorescence assays with TRF2 antibody;
- Lastly, the LAP1 knockdown experiment would also be interesting to identify possible repercussions on the DNA damage response.

Bibliography

7. References

1. Bonne, G. Nuclear envelope proteins in health and diseases. *Semin. Cell Dev. Biol.* **29,** 93–94 (2014).
2. Burke, B., Mounkes, L. C. & Stewart, C. L. The nuclear envelope in muscular dystrophy and cardiovascular diseases. *Traffic* **2,** 675–683 (2001).
3. Wilson, K. L. & Foisner, R. Lamin-binding Proteins. *Cold Spring Harb. Perspect. Biol.* **2,** 1–17 (2010).
4. Dauer, W. T. & Worman, H. J. The Nuclear Envelope as a Signaling Node in Development and Disease. *Dev. Cell* **17,** 626–638 (2009).
5. Gruenbaum, Y., Margalit, A., Goldman, R. D., Shumaker, D. K. & Wilson, K. L. The nuclear lamina comes of age. *Nat. Rev. Mol. Cell Biol.* **6,** 21–31 (2005).
6. Hetzer, M. W. The nuclear envelope. *Cold Spring Harb. Perspect. Biol.* **2,** 1–16 (2010).
7. Stanikova, D., Surova, M., Ticha, L., Petrasova, M., Virgova, D., Huckova, M., Skopkova, M., Lobotkova, D., Valentinova, L., Mokan, M., Stanik, J., Klimes, I. & Gasperikova, D. in *Physiol. Res.* **64,** 883–890 (2015).
8. Chi, Y.-H., Chen, Z.-J. & Jeang, K.-T. The nuclear envelopathies and human diseases. *J. Biomed. Sci.* **16,** 96 (2009).
9. Adam, S. A. The nuclear pore complex. *J. Cell Biol.* **2,** 977–984 (2001).
10. Ptak, C., Aitchison, J. D. & Wozniak, R. W. The multifunctional nuclear pore complex: a platform for controlling gene expression. *Curr. Opin. Cell Biol.* **28,** 147–171 (2014).
11. Hoelz, A., Debler, E. W. & Blobel, G. The Structure of the Nuclear Pore Complex. *Annu. Rev. Biochem.* **80,** 613–643 (2011).
12. Webster, B. M. & Lusk, C. P. Border Safety: Quality Control at the Nuclear Envelope. *Trends Cell Biol.* **xx,** 1–11 (2015).
13. Leksa, N. C., Brohawn, S. G. & Schwartz, T. U. The structure of the scaffold nucleoporin Nup120 reveals a new and unexpected domain architecture. *Structure* **17,** 1082–91 (2009).
14. Sood, V. & Brickner, J. H. J. J. H. Nuclear pore interactions with the genome. *Curr. Opin. Genet. Dev.* **25,** 43–49 (2014).

15. Méndez-López, I. & Worman, H. J. Inner nuclear membrane proteins: Impact on human disease. *Chromosoma* **121,** 153–167 (2012).
16. Katta, S. S., Smoyer, C. J. & Jaspersen, S. L. Destination: Inner nuclear membrane. *Trends Cell Biol.* **24,** 221–229 (2014).
17. Hirano, Y., Hizume, K., Kimura, H., Takeyasu, K., Haraguchi, T. & Hiraoka, Y. Lamin B receptor recognizes specific modifications of histone H4 in heterochromatin formation. *J. Biol. Chem.* **287,** 42654–42663 (2012).
18. Manilal, S., Nguyen, T. M., Sewry, C. A. & Morris, G. E. The Emery-Dreifuss muscular dystrophy protein, emerin, is a nuclear membrane protein. *Hum. Mol. Genet.* **5,** 801–808 (1996).
19. Wilson, K. L. & Berk, M. The nuclear envelope at a glance. *Cell Sci.* **123,** 1973–1978 (2010).
20. Heras, J. I. De, Meinke, P., Batrakou, D. G., Srsen, V., Zuleger, N., Kerr, A. R. W., Schirmer, E. C., Heras, J. I. De, Meinke, P., Batrakou, D. G., Srsen, V., Zuleger, N., Kerr, A. R. W. & Schirmer, E. C. Tissue specificity in the nuclear envelope supports its functional complexity. *Nucleus* **1034,** 460–477 (2015).
21. Broers, J. L. V, Ramaekers, F. C. S., Bonne, G., Yaou, R. Ben & Hutchison, C. J. Nuclear lamins: laminopathies and their role in premature ageing. *Physiol. Rev.* **86,** 967–1008 (2006).
22. Liu, J., Lee, K. K., Segura-Totten, M., Neufeld, E., Wilson, K. L. & Gruenbaum, Y. MAN1 and emerin have overlapping function(s) essential for chromosome segregation and cell division in Caenorhabditis elegans. *Proc. Natl. Acad. Sci. U. S. A.* **100,** 4598–4603 (2003).
23. Gonzalez, Y., Saito, A. & Sazer, S. Fission yeast Lem2 and Man1 perform fundamental functions of the animal cell nuclear lamina. *Nucleus* **3,** 60–76 (2012).
24. Lin, F., Blake, D. L., Callebaut, I., Skerjanc, I. S., Holmer, L., Mcburney, M. W., Paulin-levasseur, M. & Worman, H. J. MAN1 , an Inner Nuclear Membrane Protein That Shares the LEM Domain with Lamina-associated Polypeptide 2 and Emerin *. *Biol. Chem.* **275,** 4840–4847 (2000).
25. Brachner, A. & Foisner, R. Evolvement of LEM-proteins as chromatin tethers at the nuclear periphery. *Biochem. Soc. Trans.* **39,** 1735–1741 (2015).
26. Rebelo, S., da Cruz e Silva, E. F. & da Cruz e Silva, O. a. B. Genetic mutations

strengthen functional association of LAP1 with DYT1 dystonia and muscular dystrophy. *Mutat. Res. Mutat. Res.* 2–7 (2015). doi:10.1016/j.mrrev.2015.07.004

27. Maison, C., Pyrpasopoulou, a, Theodoropoulos, P. a & Georgatos, S. D. The inner nuclear membrane protein LAP1 forms a native complex with B-type lamins and partitions with spindle-associated mitotic vesicles. *EMBO J.* **16,** 4839–50 (1997).
28. Furukawa, K., Fritze, C. E. & Gerace, L. The major nuclear envelope targeting domain of LAP2 coincides with its lamin binding region but is distinct from its chromatin interaction domain. *J. Biol. Chem.* **273,** 4213–9 (1998).
29. Chen, Z.-J., Wang, W.-P., Chen, Y.-C., Wang, J.-Y., Lin, W.-H., Tai, L.-A., Liou, G.-G., Yang, C.-S. & Chi, Y.-H. Dysregulated interactions between lamin A and SUN1 induce abnormalities in the nuclear envelope and endoplasmic reticulum in progeric laminopathies. *J. Cell Sci.* **127,** 1792–804 (2014).
30. Cartwright, S. & Karakesisoglou, I. Nesprins in health and disease. *Semin. Cell Dev. Biol.* **29,** 169–179 (2014).
31. Worman, H. J. & Dauer, W. T. The Nuclear Envelope: An Intriguing Focal Point for Neurogenetic Disease. *Neurotherapeutics* **11,** 764–772 (2014).
32. Zhang, Q., Skepper, J. N., Yang, F., Davies, J. D., Hegyi, L., Roberts, R. G., Weissberg, P. L., Ellis, J. a & Shanahan, C. M. Nesprins: a novel family of spectrin-repeat-containing proteins that localize to the nuclear membrane in multiple tissues. *J. Cell Sci.* **114,** 4485–4498 (2001).
33. Libotte, T., Zaim, H., Abraham, S, Pasmakumar, V. C., Schneider, M., Lu, W., Munck, M., Hutchison, C., Wehnert, M., Fahrenkrog, B., Sauder, U., Aebi, U., Noegel, A. A., Karakesisoglou, I. Lamin A/C–dependent Localization of Nesprin-2, a Giant Scaffolder at the Nuclear Envelope. *Mol. Biol. Cell* **16,** 1–13 (2005).
34. Wilhelmsen, K. Nesprin-3, a novel outer nuclear membrane protein, associates with the cytoskeletal linker protein plectin. *J. Cell Biol.* **171,** 799–810 (2005).
35. Roux, K. J., Crisp, M. L., Liu, Q., Kim, D., Kozlov, S., Stewart, C. L. & Burke, B. Nesprin 4 is an outer nuclear membrane protein that can induce kinesin-mediated cell polarization. *Proc. Natl. Acad. Sci. U. S. A.* **106,** 2194–2199 (2009).
36. Shin, J. Y., Dauer, W. T. & Worman, H. J. Lamina-associated polypeptide 1: Protein interactions and tissue-selective functions. *Semin. Cell Dev. Biol.* **29,** 164–168 (2014).
37. Santos, M., Rebelo, S., Van Kleeff, P. J. M., Kim, C. E., Dauer, W. T., Fardilha, M.,

da Cruz e Silva, O. A. & da Cruz e Silva, E. F. The Nuclear Envelope Protein, LAP1B, Is a Novel Protein Phosphatase 1 Substrate. *PLoS One* **8,** 1–13 (2013).

38. Santos, M., Domingues, S. C., Costa, P., Muller, T., Galozzi, S., Marcus, K., da Cruz e Silva, E. F., da Cruz e Silva, O. a. & Rebelo, S. Identification of a Novel Human LAP1 Isoform That Is Regulated by Protein Phosphorylation. *PLoS One* **9,** e113732 (2014).
39. Rebelo, S., Da Cruz e Silva, E. F. & Da Cruz e Silva, O. A. B. Genetic mutations strengthen functional association of LAP1 with DYT1 dystonia and muscular dystrophy. *Mutat. Res. - Rev. Mutat. Res.* **766,** 42–47 (2015).
40. Santos, M., Costa, P., Martins, F., da Cruz e Silva, E. F., da Cruz e Silva, O. a. B. & Rebelo, S. LAP1 is a crucial protein for the maintenance of the nuclear envelope structure and cell cycle progression. *Mol. Cell. Biochem.* **399,** 143–153 (2014).
41. Graça, M. S. M. Characterization of novel LAP1 complexes and their relevance in DYT1 dystonia. (2014).
42. Granata, a. & Warner, T. T. The role of torsinA in dystonia. *Eur. J. Neurol.* **17,** 81–87 (2010).
43. Naismith, T. V, Heuser, J. E., Breakefield, X. O. & Hanson, P. I. TorsinA in the nuclear envelope. *Proc. Natl. Acad. Sci. U. S. A.* **101,** 7612–7 (2004).
44. Shin, J., Méndez-lópez, I., Wang, Y., Hays, A. P., Tanji, K., Lefkowitch, J. H., Schulze, P. C., Worman, H. J. & Dauer, W. T. Lamina-associated Polypeptide-1 Interacts with the Muscular Dystrophy Protein Emerin and is Essential for Skeletal Muscle Maintenance. *Dev. Cell* **26,** 591–603 (2013).
45. Serrano, J., da Cruz e Silva, O. & Rebelo, S. Lamina Associated Polypeptide 1 (LAP1) Interactome and Its Functional Features. *Membranes (Basel).* **6,** 8 (2016).
46. Kayman-Kurekci, G., Talim, B., Korkusuz, P., Sayar, N., Sarioglu, T., Oncel, I., Sharafi, P., Gundesli, H., Balci-Hayta, B., Purali, N., Serdaroglu-Oflazer, P., Topaloglu, H. & Dincer, P. Mutation in TOR1AIP1 encoding LAP1B in a form of muscular dystrophy: a novel gene related to nuclear envelopathies. *Neuromuscul. Disord.* **24,** 624–33 (2014).
47. Dorboz, I., Coutelier, M., Bertrand, A. T., Caberg, J.-H., Elmaleh-Bergès, M., Lainé, J., Stevanin, G., Bonne, G., Boespflug-Tanguy, O. & Servais, L. Severe dystonia, cerebellar atrophy, and cardiomyopathy likely caused by a missense mutation in

TOR1AIP1. *Orphanet J. Rare Dis.* **9,** 174 (2014).

48. Ghaoui, R., Benavides, T., Lek, M., Waddell, L. B., Kaur, S., North, K. N., MacArthur, D. G., Clarke, N. F. & Cooper, S. T. TOR1AIP1 as a cause of cardiac failure and recessive limb-girdle muscular dystrophy. *Neuromuscul. Disord.* **26,** 500–503 (2016).
49. Sosa, B. a, Demircioglu, F. E., Chen, J. Z., Ingram, J., Ploegh, H. L. & Schwartz, T. U. How lamina-associated polypeptide 1 (LAP1) activates Torsin. *Elife* **3,** e03239 (2014).
50. Bonne, Á., Schwartz, K. & Helbling-leclerc, A. Emery-Dreifuss muscular dystrophy. *Eur. J. Hum. Genet.* **10,** 157–161 (2002).
51. Bione, S., Maestrini, E., Rivella, S., Mancini, M., Regis, S., Romeo, G. & Toniolo, D. Identification of a novel X-linked gene responsible for Emery-Dreifuss muscular dystrophy. *Nat. Genet.* **8,** 323–327 (1994).
52. Nagano, A., Koga, R., Ogawa, M., Kurano, Y., Kawada, J., Okada, R., Hayashi, Y. K., Tsukahara, T., A. K. Emerin deficiency at the nuclear membrane in patients with Emery- Dreifuss muscular dystrophy. *Nat Genet.* **14,** 353–6 (1996).
53. Jackson, S. P. & Bartek, J. The DNA-damage response in human biology and disease. *Nature* **461,** 1071–1078 (2010).
54. Uryga, A., Gray, K. & Bennett, M. DNA Damage and Repair in Vascular Disease. *Annu. Rev. Phisiology* **78,** 45–66 (2016).
55. Polo, S. & Jackson, S. Dynamics of DNA damage response proteins at DNA breaks: a focus on protein modifications. *Genes Dev.* **25,** 409–33 (2011).
56. Liu, Y., Li, Y. & Lu, X. Regulators in the DNA Damage Response. *Arch. Biochem. Biophys.* **594,** 18–25 (2016).
57. Kurz, E. U. & Lees-Miller, S. P. DNA damage-induced activation of ATM and ATM-dependent signaling pathways. *DNA Repair (Amst).* **3,** 889–900 (2004).
58. Ciccia, A. & Elledge, S. J. The DNA Damage Response: Making It Safe to Play with Knives. *Mol. Cell* **40,** 179–204 (2010).
59. Hill, C. & Carolina, N. ATR Kinase Inhibition Protects Non-cycling Cells from the Lethal Effects of DNA Damage and Transcription Stress. *J. Biol. Chem.* **291,** 9330–9354 (2016).
60. Olcina, M. M. & Hammond, E. M. in *Hypoxia Cancer Biol. Implic. Ther. Oppor.* 21–

30 (2014). doi:10.1007/978-1-4614-9167-5

61. Freeman, A. K. & Monteiro, A. N. Phosphatases in the cellular response to DNA damage. *Cell Commun. Signal.* **8,** 27 (2010).

62. Zhou, B. S., Bartek, J. & Road, H. C. TARGETING THE CHECKPOINT KINASES: CHEMOSENSITIZATION VERSUS CHEMOPROTECTION. *Nat. Rev. Cancer* **4,** 1–10 (2004).

63. Sulli, G. & Micco, R. Di. Crosstalk between chromatin state and DNA damage response in cellular senescence and cancer. *Nat. Rev. Cancer* **12,** 709–720 (2012).

64. Arishya Sharma , Kamini Singh, and A. A. *Histone H2AX Phosphorylation: A Marker for DNA Damage*. *DNA Repair Protoc. Methods Mol. Biol.* **920,** (2012).

65. Ding, B., Chi, S. G., Kim, S. H., Kang, S., Cho, J. H., Kim, D. S. & Cho, N. H. Role of p53 in antioxidant defense of HPV-positive cervical carcinoma cells following H2O2 exposure. *J. Cell Sci.* **120,** 2284–2294 (2007).

66. Chen, K., Albano, A., Ho, A. & Keaney, J. F. Activation of p53 by oxidative stress involves platelet-derived growth factor-B receptor-mediated Ataxia Telangiectasia Mutated (ATM) kinase activation. *J. Biol. Chem.* **278,** 39527–39533 (2003).

67. Oeseburg, H., De Boer, R. A., Van Gilst, W. H. & Van Der Harst, P. Telomere biology in healthy aging and disease. *Pflugers Arch. Eur. J. Physiol.* **459,** 259–268 (2010).

68. Houben, J. M. J., Moonen, H. J. J., van Schooten, F. J. & Hageman, G. J. Telomere length assessment: Biomarker of chronic oxidative stress? *Free Radic. Biol. Med.* **44,** 235–246 (2008).

69. Wong, L. S. M., Van Der Harst, P., De Boer, R. A., Huzen, J., Van Gilst, W. H. & Van Veldhuisen, D. J. Aging, telomeres and heart failure. *Heart Fail. Rev.* **15,** 479–486 (2010).

70. Lu, W., Zhang, Y., Liu, D., Songyang, Z. & Wan, M. Telomeres-structure, function, and regulation. *Exp. Cell Res.* **319,** 133–141 (2013).

71. Lee, O.-H., Kim, H., He, Q., Baek, H. J., Yang, D., Chen, L.-Y., Liang, J., Chae, H. K., Safari, A., Liu, D. & Songyang, Z. Genome-wide YFP fluorescence complementation screen identifies new regulators for telomere signaling in human cells. *Mol. Cell. Proteomics* **10,** M110.001628 (2011).

72. Zhu, H., Belcher, M. & van der Harst, P. Healthy aging and disease: role for telomere biology? *Clin. Sci. (Lond).* **120,** 427–440 (2011).

73. Young, N. S. Telomere biology and telomere diseases: implications for practice and research. *Hematology Am. Soc. Hematol. Educ. Program* **2010,** 30–35 (2010).

74. Dunham, M. A., Neumann, A. A., Fasching, C. L. & Reddel, R. R. Telomere maintenance by recombination in human cells. *Nat. Genet.* **26,** 447–450 (2000).

75. Lange, T. How Telomeres Solve the End-Protection Problem. *Science (80-.).* **326,** 1–13 (2009).

76. Kim, S. H., Kaminker, P. & Campisi, J. TIN2, a new regulator of telomere length in human cells. *Nat. Genet.* **23,** 405–412 (1999).

77. Liu, D., O'Connor, M. S., Qin, J. & Songyang, Z. Telosome, a mammalian telomere-associated complex formed by multiple telomeric proteins. *J. Biol. Chem.* **279,** 51338–51342 (2004).

78. de Lange, T. Protection of mammalian telomeres. *Oncogene* **21,** 532–40 (2002).

79. Okamoto, K., Bartocci, C., Ouzounov, I., K.Diedrich, J., Ill, J. R. Y. & Denchi, E. L. A two-step mechanism for TRF2-mediated chromosome end protection. *Nature* **494,** 502–505 (2013).

80. Martínez, P., Ferrara-Romeo, I., Flores, J. M. & Blasco, M. A. Essential role for the TRF2 telomere protein in adult skin homeostasis. *Aging Cell* **13,** 656–668 (2014).

81. Janoušková, E., Nečasová, I., Pavloušková, J., Zimmermann, M., Hluchý, M., Marini, V., Nováková, M. & Hofr, C. Human Rap1 modulates TRF2 attraction to telomeric DNA. *Nucleic Acids Res.* **43,** 2691–700 (2015).

82. Agnel Sfeir, Shaheen Kabir, Megan van Overbeek, Giulia B. Celli, and T. de L. Loss of Rap1 induces telomere recombination in absence of NHEJ or a DNA damage signal. *Science.* **18,** 1199–1216 (2013).

83. Celli, G. B. & de Lange, T. DNA processing is not required for ATM-mediated telomere damage response after TRF2 deletion. *Nat. Cell Biol.* **7,** 712–8 (2005).

84. Huda, N., Tanaka, H., Mendonca, M. S. & Gilley, D. DNA damage-induced phosphorylation of TRF2 is required for the fast pathway of DNA double-strand break repair. *Mol. Cell. Biol.* **29,** 3597–604 (2009).

85. Karlseder, J., Hoke, K., Mirzoeva, O. K., Bakkenist, C., Kastan, M. B., Petrini, J. H. J. & De Lange, T. The telomeric protein TRF2 binds the ATM Kinase and Can Inhibit the ATM-dependent DNA damage response. *PLoS Biol.* **2,** 1150–1156 (2004).

86. Huda, N., Abe, S., Gu, L., Mendonca, M. S., Mohanty, S. & Gilley, D. Recruitment

of TRF2 to laser-induced DNA damage sites. *Free Radic. Biol. Med.* **53,** 1192–1197 (2012).

87. Bradshaw, P. S., Stavropoulos, D. J. & Meyn, M. S. Human telomeric protein TRF2 associates with genomic double-strand breaks as an early response to DNA damage. *Nat. Genet.* **37,** 193–7 (2005).
88. Goodchild, R. E. & Dauer, W. T. The AAA+ protein torsinA interacts with a conserved domain present in LAP1 and a novel ER protein. *J. Cell Biol.* **168,** 855–62 (2005).
89. Pallepati, P. & Averill-bates, D. A. Biochimica et Biophysica Acta Activation of ER stress and apoptosis by hydrogen peroxide in HeLa cells : Protective role of mild heat preconditioning at 40 ° C. *BBA - Mol. Cell Res.* **1813,** 1987–1999 (2011).
90. Lin, G. G. & Scott, J. G. Functional interplay between ATM/ATR-mediated DNA damage response and DNA repair pathways in oxidative stress. *Cell Mol. life Sci.* **100,** 130–134 (2014).
91. Cummings, B. S., Wills, L. P. & Schnellmann, R. G. Measurement of Cell Death in Mammalian Cells. *Curr Protoc Phamacol* **1,** 1–30 (2004).
92. Ampules, A. S. Pierce BCA Protein Assay Kit. **747,** (2000).
93. LiCor. Odyssey Infrared Imaging System. *Biosciences* 1–211 (2009).
94. Burry, R. W. *Immunocytochemistry: A practical guide for biomedical research*. *Springer* (2010). doi:10.1007/978-1-4419-1304-3
95. GraphPad Software Inc. GraphPad Statistics Guide. *GraphPad* 2015 (2012).
96. Brückner, A., Polge, C., Lentze, N., Auerbach, D. & Schlattner, U. Yeast Two-Hybrid , a Powerful Tool for Systems Biology. *Int. Jounal Mol. Sci.* **10,** 2763–2788 (2009).
97. Bilaud, T., Brun, C., Ancelin, K., Koering, C. E., Laroche, T. & Gilson, E. Telomeric localization of TRF2, a novel human telobox protein. *Nat. Genet.* **17,** 236–9 (1997).
98. Jung, Y., Lee, S., Bang, S., Kim, S., Choi, K., Lee, C., Lee, S. G., Kim, C. J., Song, K. & Lee, I. TRF2 is in neuroglial cytoplasm and induces neurite-like processes. *FEBS Lett.* **557,** 129–132 (2004).
99. Podhorecka, M., Skladanowski, A. & Bozko, P. H2AX Phosphorylation: Its Role in DNA Damage Response and Cancer Therapy. *J. Nucleic Acids* **2011,** 1–9 (2011).
100. Ermler, S., Krunic, D., Knoch, T. a, Moshir, S., Mai, S., Greulich-Bode, K. M. & Boukamp, P. Cell cycle-dependent 3D distribution of telomeres and telomere repeat-

binding factor 2 (TRF2) in HaCaT and HaCaT-myc cells. *Eur. J. Cell Biol.* **83,** 681–90 (2004).

101. Xin, H., Liu, D. & Songyang, Z. The telosome/shelterin complex and its functions. *Genome Biol.* **9,** 232 (2008).
102. Chowdhury, D., Keogh, M.-C., Ishii, H., Peterson, C. L., Buratowski, S. & Lieberman, J. γ-H2AX dephosphorylation by protein phosphatase 2A facilitates DNA double-strand break repair. *Mol. Cell* **20,** 801–809 (2005).
103. Miller, K. M., Ferreira, M. G. & Cooper, J. P. Taz1, Rap1 and Rif1 act both interdependently and independently to maintain telomeres. *EMBO J.* **24,** 3128–3135 (2005).
104. Singh, M., Sharma, H. & Singh, N. Hydrogen peroxide induces apoptosis in HeLa cells through mitochondrial pathway. *Mitochondrion* **7,** 367–373 (2007).
105. Schwartz, E. I., Smilenov, L. B., Price, M. A., Osredkar, T., Baker, R. A., Ghosh, S., Shi, F. D., Vollmer, T. L., Lencinas, A., Stearns, D. M., Gorospe, M. & Kruman, I. I. Cell cycle activation in postmitotic neurons is essential for DNA repair. *Cell Cycle* **6,** 318–329 (2007).
106. Arnone, J. T., Walters, A. D. & Cohen-fix, O. The dynamic nature of the nuclear envelope. *Nucleus* **4,** 261–266 (2013).
107. Güttinger, S., Laurell, E. & Kutay, U. Orchestrating nuclear envelope disassembly and reassembly during mitosis. *Nat. Rev. Mol. Cell Biol.* **10,** 178–191 (2009).
108. Zhang, S., Hemmerich, P. & Grosse, F. Nucleolar localization of the human telomeric repeat binding factor 2 (TRF2). *J. Cell Sci.* **117,** 3935–3945 (2004).
109. Yang, L., Cuan, T. & Gerace, L. Integral membrane proteins ofthe nuclear envelope are dispersed throughout the endoplasmic reticulumduring mitosis. *J. Cell Biol.* **137,** 1199–1210 (1997).
110. Gerace, L. & Foisner, R. Integral membrane proteins and dynamic organization of the nuclear envelope. *Trends Cell Biol.* **4,** 127–131 (1994).
111. Ilicheva, N. V., Podgornaya, O. I. & Voronin, A. P. *Telomere Repeat-Binding Factor 2 Is Responsible for the Telomere Attachment to the Nuclear Membrane*. *Adv. Protein Chem. Struct. Biol.* **101,** (Elsevier Inc., 2015).

Appendix 1

Statistical analysis

A. Effects of H_2O_2 on the cell growth in HeLa cells

One-way ANOVA	p-value
Multiple comparisons test-Dunnets	
0 μM vs 80 μM (12 hours)	*

B. Percentage of apoptotic cells

One-way ANOVA	p-value
Multiple comparisons test-Dunnets	
0 μM vs 20 μM (6 hours)	#
0 μM vs 40 μM (6 hours)	#
0 μM vs 80 μM (6 hours)	#
0 μM vs 80 μM (12 hours)	*

C. Evaluate the expression levels of the LAP1:TRF2 complex during DNA damage

I. Expression levels of LAP1

One-way ANOVA	p-value
Multiple comparisons test-Dunnets	
0 μM vs 80 μM (12 hours)	*
20 μM (0 hours vs 12 hours)	#

II. Expression levels of TRF2

One-way ANOVA	p-value
Multiple comparisons test-Dunnets	
0 μM vs 20 μM (6 hours)	*
0 μM vs 40 μM (6 hours)	*
0 μM vs 20 μM (12 hours)	#
0 μM vs 40 μM (12 hours)	#

D. Evaluation of the subcellular distribution of LAP1 and TRF2 during DNA damage

t-test	p-value
0 μM vs 80 μM (12 hours)	*

Appendix 2

Culture media and Solutions

I. Cell culture Solutions

- **PBS (1x)**

For a final volume of 500 mL, dissolve one pack of BupH Modified Dulbecco's Phosphate Buffered Saline Pack (Pierce) in deionized H_2O. Final composition:

  - 8 mM Sodium Phosphate
  - 2 mM Potassium Phosphate
  - 140 mM Sodium Chloride
  - 10 mM Potassium Chloride

Sterilize by filtering through a 0.2 μm filter and store at 4°C.

- **10% FBS MEM: F12 (1:1)**
  - 4.805 g MEM
  - 5.315 g F12
  - 1.5 g NaHCO3
  - 0.055 g Sodium Pyruvate
  - 10 mL Streptomycin/Penicillin/Amphotericin solution
  - 100 mL 10% FBS
  - 2.5 mL L-glutamine (200 mM stock solution)

Dissolve in deionized H_2O. Adjust the pH to 7.2-7.3. Adjust the volume to 1000 mL with deionized H_2O.

- **10% FBS DMEM**

  -13.4 g DMEM

  -3.7 g $NaHCO_3$

  - 10 mL Streptomycin/Penicillin/Amphotericin solution (AAs)

  - 100 mL 10% FBS

Dissolve in deionized H_2O. Adjust the pH to 7.2-7.3. Adjust the volume to 1000 mL with deionized H_2O.

II. Western Blot Solutions

- **LGB (lower gel buffer) (4x)**

To 900 mL of deionized H_2O add:

- 181.65 g of Tris
- 4 g of SDS

Mix until the solutes have dissolved. Adjust pH to 8.9 and adjust the volume to 1 L with deionized H_2O.

- **UGB (Upper gel buffer) (4x)**

To 900 mL of deionized H_2O add:

- 75.69 g of Tris

Mix until the solute has dissolved. Adjust the pH to 6.8 and adjust the volume to 1 L with deionized H_2O.

- **10% APS (ammonium persulfate)**

In 10 mL of deionized H_2O dissolve 1 g of APS. Note: prepare fresh before use.

- **10% SDS (sodium dodecilsulfate)**

In 10 mL of deionized H_2O dissolve 1 g of SDS.

- **Loading Gel Buffer (4x)**
  - 2.5 mL 1M Tris solution (pH 6.8) 2.5 mL (250 mM)
  - 0.8 g SDS (8%)
  - 4 mL Glicerol (40%)
  - 2 mL β-mercaptoethanol (2%)
  - 1 mg Bromofenol blue (0.01%)

Adjust the volume to 10 mL with deionized H_2O. Store in darkness at room temperature.

- **1 M Tris (pH 6.8) solution**

To 150 mL of deionized H_2O add:

  - 30.3 g Tris base

Adjust the pH to 6.8 and adjust the final volume to 250 mL with deionized H_2O.

- **10x Running Buffer**
  - 30.3 g Tris (250 mM)
  - 144.2 g Glycine (2.5 M)
  - 10 g SDS (1%)

  Dissolve in deionized H_2O, adjust the pH to 8.3 and adjust the volume to 1L.

- **Stacking and resolving gel**

Components	Running gel (7.5 %)	Running gel (5%)	Running gel (20 %)	Stacking gel (3.5%)
Water	16.71 mL	9.29 mL	3.67 mL	3.3 mL
40% Acrylamide: Bis Acrylamide (29:1)	5.63 mL	1.875 mL	7.5 mL	0.6 mL
4x LGB	7.5 mL	3.75 mL	3.75 mL	---------- -
5x UGB	---------- -	---------- -	---------- -	1.0 mL
10% SDS	---------- -	---------- -	---------- -	50 µL
10% APS	150 µL	75 µL	75 µL	50 µL
TEMED	15 µL	7.5 µL	7.5 µL	5 µL

- **Transfer Buffer (1x)**
  - 3.03 g Tris (25 mM)
  - 14.41 g Glycine (192 mM)

Mix until solutes dissolution. Adjust the pH to 8.3 with HCl and adjust the volume to 800 mL with deionized H_2O. Just prior to use add 200 mL of methanol (20%).

- **10x TBS (Tris buffered saline)**
  - 12.11 g Tris (10 mM)
  - 87.66 g NaCl (150 mM)

Adjust the pH to 8.0 with HCl and adjust the volume to 1 l with deionized H_2O.

- **10x TBST (TBS+Tween)**
  - 12.11 g Tris (10 mM)
  - 87.66 g NaCl (150 mM)
  - 10 mL Tween-20 (0.01%)

Adjust the pH to 8.0 with HCl and adjust the volume to 1 L with deionized H_2O.

III. Immunofluorescence Solutions

- **4% Paraformaldehyde**

For a final volume of 100 mL, add 4 g of paraformaldehyde to 25 mL deionized H_2O. Dissolve by heating the mixture at 58°C while stirring. Add 1-2 drops of 1 M NaOH to clarify the solution and filter through a 0.2 μM filter. Add 50 mL of 2x PBS and adjust the volume to 100 mL with deionized H_2O.

IV. H_20_2 treatment

- **10 mM H_20_2 (stock solution)**

Hydrogen peroxide (98% purity) from Acros Organic was dissolved in deionized water to produce a 10 Mm stock solution.